Science of the Total Environment 736 (2020) 139588

Contents lists available at ScienceDirect

Science of the Total Environment

journal homepage: www.elsevier.com/locate/scitotenv

Anaerobic oxidation of methane and associated microbiome in anoxic water of Northwestern Siberian lakes

Léa Cabrol [a,h,i], Frédéric Thalasso [b], Laure Gandois [c], Armando Sepulveda-Jauregui [d,e], Karla Martinez-Cruz [d], Roman Teisserenc [c], Nikita Tananaev [f], Alexander Tveit [g], Mette M. Svenning [g], Maialen Barret [c,*]

[a] Aix-Marseille University, Univ Toulon, CNRS, IRD, M.I.O. UM 110, Mediterranean Institute of Oceanography, Marseille, France
[b] Biotechnology and Bioengineering Department, Center for Research and Advanced Studies (Cinvestav), Mexico City, Mexico
[c] Laboratory of Functional Ecology and Environment, Université de Toulouse, CNRS, Toulouse, France
[d] ENBEELAB, University of Magallanes, Punta Arenas, Chile
[e] Center for Climate and Resilience Research (CR)2, Santiago, Chile
[f] Melnikov Permafrost Institute, Yakutsk, Russia
[g] Department of Arctic and Marine Biology, UiT The Arctic University of Norway, Tromsø, Norway
[h] Institute of Ecology and Biodiversity IEB, Faculty of Sciences, Universidad de Chile, Santiago, Chile
[i] Escuela de Ingeniería Bioquímica, Pontificia Universidad de Valparaiso, Av Brasil 2085, Valparaiso, Chile

HIGHLIGHTS

- Anaerobic oxidation of CH_4 (AOM) was a major sink in the water of 4 Siberian lakes.
- AOM mitigated 60–100% of the produced CH_4.
- All four lakes shared the same predominant methanotrophs in AOM hotspots.
- AOM was attributed to *Methylobacter* and other *Methylomonadaceae*.
- Methanotrophs co-occurred with denitrifiers and iron-cycling partners.

GRAPHICAL ABSTRACT

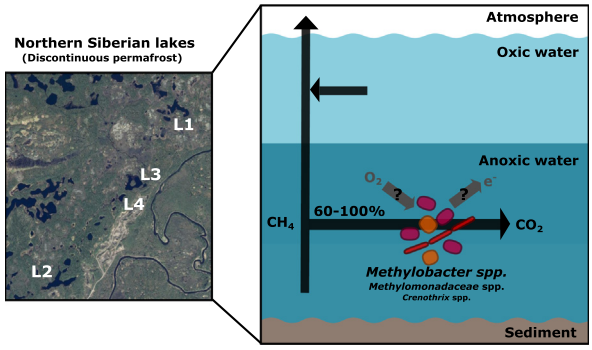

ARTICLE INFO

Article history:
Received 19 February 2020
Received in revised form 7 May 2020
Accepted 19 May 2020
Available online 25 May 2020

Editor: Ewa Korzeniewska

Keywords:
Arctic
Anaerobic oxidation of methane
Methanotroph
Methylomonadaceae
Methylobacter
Permafrost

ABSTRACT

Arctic lakes emit methane (CH_4) to the atmosphere. The magnitude of this flux could increase with permafrost thaw but might also be mitigated by microbial CH_4 oxidation. Methane oxidation in oxic water has been extensively studied, while the contribution of anaerobic oxidation of methane (AOM) to CH_4 mitigation is not fully understood. We have investigated four Northern Siberian stratified lakes in an area of discontinuous permafrost nearby Igarka, Russia. Analyses of CH_4 concentrations in the water column demonstrated that 60 to 100% of upward diffusing CH_4 was oxidized in the anoxic layers of the four lakes. A combination of *pmoA* and *mcrA* gene qPCR and 16S rRNA gene metabarcoding showed that the same taxa, all within *Methylomonadaceae* and including the predominant genus *Methylobacter* as well as *Crenothrix*, could be the major methane-oxidizing bacteria (MOB) in the anoxic water of the four lakes. Correlation between *Methylomonadaceae* and OTUs within *Methylotenera*, *Geothrix* and *Geobacter* genera indicated that AOM might occur in an interaction between MOB, denitrifiers and iron-cycling partners. We conclude that MOB within *Methylomonadaceae* could have a crucial impact on CH_4 cycling in these Siberian Arctic lakes by mitigating the majority of produced CH_4 before it leaves the anoxic zone. This finding emphasizes the importance of AOM by *Methylomonadaceae* and extends our knowledge about CH_4 cycle in lakes, a crucial component of the global CH_4 cycle.

* Corresponding author.
E-mail address: maialen.barret@ensat.fr (M. Barret).

https://doi.org/10.1016/j.scitotenv.2020.139588

1. Introduction

High-latitude lakes, mostly located in permafrost-dominated area (Smith et al., 2007), are major sources of methane (CH_4) to the atmosphere. It has been estimated that lakes located above 50° of northern latitude are responsible for 18.8 Tg y^{-1}, i.e. 26% of total lake CH_4 emissions that are estimated to 71 Tg y^{-1} (Saunois et al., 2019). Lake CH_4 emissions represent about 19% of non-anthropogenic global CH_4 sources in bottom-up estimations. According to the International Panel on Climate Change (IPCC, 2013), the global mean surface temperatures are projected to increase between 1.7 °C and 4.8 °C by 2100 and the climate is changing twice as fast in the Arctic (Cohen et al., 2014). Under the global warming scenario of +2 °C, the reduction of permafrost area by 40% due to thawing (Chadburn et al., 2017) will disturb the arctic biome hydrology through lake and pond formation, expansion, and drainage (Vonk et al., 2015). Permafrost region comprises 50% of the global soil organic carbon stock (Hugelius et al., 2014; Strauss et al., 2017) and therefore future thawing is likely to shift the balance of the global carbon cycle by making organic carbon available to microbial decomposition and conversion into CH_4 (McGuire et al., 2009; Wik et al., 2016). From the global mean radiative forcing of 2.83 W m^{-2} for well mixed greenhouse gases, CO_2, CH_4 and N_2O represent 64%, 17% and 6%, respectively (Myhre et al., 2013). However, when considering aquatic waterbodies (lakes and impoundments), the individual contributions of CH_4, CO_2 and N_2O to total radiative forcing range between 71.8 and 77.8%, 19.6 and 26.1%, and 2.0 and 2.6%, showing that CH_4 emissions in these ecosystems have the highest positive feedback on global warming (DelSontro et al., 2018a). Thus the microorganisms and metabolic pathways controlling CH_4 emissions must be better constrained in order to understand the link between changing Arctic permafrost ecosystems and global climate (Boetius, 2019; Singh et al., 2010).

Biogenic CH_4 production by methanogenesis in lakes occurs primarily under highly reduced conditions in the sediments where organic matter is decomposed, while emissions of CH_4 from lake sediments to the atmosphere are significantly mitigated by CH_4 oxidation in the water column (Bastviken et al., 2008). Aerobic CH_4 oxidation is carried out by methane-oxidizing bacteria (MOB) using CH_4 as a carbon and energy source, the initial step of CH_4 oxidation being catalyzed by the methane monooxygenase enzyme. Aerobic MOB belong to three lineages, γ-Proteobacteria, α-Proteobacteria and Verrucomicrobia, with different carbon assimilation pathways (Knief, 2015). Using genome-based taxonomic classification, the MOB within γ-Proteobacteria (γ-MOB) were recently reassigned to three families, *Methylococcaceae*, *Methylomonadaceae* and *Methylothermaceae* (Parks et al., 2018). Most γ-MOB grow solely on CH_4, some also on its C1-derivative methanol (Chistoserdova and Lidstrom, 2013). MOB within α-Proteobacteria that were formerly assigned to the families *Methylocystaceae* and *Beijerinckiaceae* have recently been merged into *Beijerinckiaceae* (Parks et al., 2018). The *Beijerinckiaceae* lineage includes obligate and facultative MOB, which grow primarily on CH_4 but also a range of methyl- and multi-carbon substrates (Khmelenina et al., 2018; Tamas et al., 2014). The third group of MOB belongs to the *Methylacidiphilaceae* family within Verrucomicrobia and use methane only as an energy source while fixing CO_2 for cell synthesis through the Calvin-Benson-Bassham pathway (Khmelenina et al., 2018).

The understanding of the CH_4 cycling in freshwater ecosystems based on methane production in sediments and methane oxidation in oxic water has been substantially improved over the last decades with the discovery of (i) methane production in oxic layers (Bogard et al., 2014; Grossart et al., 2011; Schulz et al., 2001) and (ii) anaerobic oxidation of methane (AOM). AOM activity was reported decades ago in lake water samples (Panganiban et al., 1979) and marine or freshwater sediments (Barnes and Goldberg, 1976; Zehnder and Brock, 1980). In sediments, AOM can be carried out by anaerobic methane-oxidizing archaea (ANME) within the class Methanomicrobia (Joye, 2012; Knittel and Boetius, 2009; Shen et al., 2019; Valentine et al., 2000; Winkel et al., 2019) that couple CH_4 oxidation with the reduction of sulfate, nitrate, nitrite, metal oxides or organic matter (Joye, 2012; Thauer, 2010; Valenzuela et al., 2019). Beside, AOM can also be carried out by Bacteria, attributed to *Candidatus* Methylomirabilis (NC10 phylum) through CH_4 oxidation catalyzed by the methane monooxygenase enzyme, coupled to nitrite dismutation, i.e. production of intracellular oxygen used to aerobically oxidize CH_4 (Ettwig et al., 2010). In anoxic water, NC10 clade dominated the microbial community in two lakes (Graf et al., 2018; Mayr et al., 2019). A few studies reported the prevalence and activity of presumably aerobic γ-MOB in anoxic waters (van Grinsven et al., 2020; Milucka et al., 2015; Oswald et al., 2016b, 2015; Rissanen et al., 2018). Out of four lakes, a niche-partitioning analysis conducted on methane-oxidizing bacteria concluded that some strains within *Crenothrix* and *Methylobacter* (Methylococcales) preferred oxygen-deficient conditions (Mayr et al., 2019). MOB could survive for a certain time under anoxic conditions without being active, between intermittent periods of O_2 availability (Blees et al., 2014). The micro-aerobic MOB *Methylospira mobilis* (*Methylococcaceae*) has been recently isolated from northern wetland and shows adaptation to micro-oxic habitats. Its survival capacity to a wide range of O_2 concentrations has been attributed to low- and high-affinity oxidases (Oshkin et al., 2019). The recently proposed mechanisms underlying the hypoxia stress response in *Methylobacter* involve a complex interconnection between nitric oxide reductase, quorum sensing, the secondary metabolite tundrenone, and methanol dehydrogenase functions (Yu et al., 2020). Until now, MOB activity has been evidenced in hypoxic and microaerobic pure cultures, but not in strictly anaerobic ones, to our knowledge. However, the metabolic basis and origin of oxygen for AOM by aerobic MOB within interacting microbiomes, has not been described. Furthermore, the contribution of this puzzling phenomenon to the CH_4 budgets in lakes remains to be estimated.

A Northern Siberian lake in which the methane oxidation rate in the anoxic water was high enough to fully mitigate the CH_4 flux from the bottom was recently reported (Thalasso et al., 2020). Here, we show that AOM substantially mitigated CH_4 in the anoxic waters of three neighbouring stratified lakes. By combining CH_4 diffusion-reaction modelling with in-depth analysis of the microbial key players, we provide the first evidence that *Methylomonadaceae* could act as a major CH_4 sink in anoxic lake water.

2. Material and methods

2.1. Field sites

Four stratified glacial lakes under thermokarstic influence were sampled in August 2016 (L1, L2, L3, L4) around Igarka, Russia (67.465°N, 86.578°E), on the eastern bank of the Yenisei river. The lakes are located in a discontinuous permafrost area (Streletsky et al., 2015) characterized by a patchwork of boreal forest, lakes and peatlands, including palsa complexes. Annual mean temperature is 8.3 °C, the annual precipitation is 495 mm and the elevation is around 55 m AMSL. The lake areas ranged from 0.7 to 6.5 ha, and the lake maximum depths ranged from 6 to 12 m.

2.2. In situ physico-chemical characterization

Before sampling, the water column was characterized at the center of the lakes at two replicate locations a few meters apart (A, B). Since L2 is formed by two distinct basins (Thalasso et al., 2020), a location from the second basin was added, approximately 200 m to the west and called location D. Dissolved oxygen (DO), with a detection limit of 10 μg L^{-1}, temperature, pH, conductivity and redox potential were measured with a multiparametric probe (HI 9828, Hanna Instrument, Woonsocket, RI, US).

Dissolved CH_4 concentrations along the water column were determined using a membrane-integrated cavity output spectrometry (M-ICOS) method (Gonzalez-Valencia et al., 2014). This method, described in more detail in the Supplementary material, is based on a gas-liquid equilibration module. Briefly, a continuous flow of water, pumped from the desired depth of the water column, is forced to equilibrate with a continuous flow of CH_4- and CO_2-free nitrogen, which is then measured with an ultraportable greenhouse gas analyzer (UGGA; Model 30P, Los Gatos Research, San Jose, CA, USA). After proper calibration, this method allowed for the continuous measurement of dissolved CH_4 at high-resolution, with a frequency of 1 s^{-1}. Thus, a weighted probe containing a water filter and connected to a water pump and the M-ICOS device was continuously lowered at constant speed, trough the water column, which allowed for about 50 dissolved CH_4 concentration data points per meter of water column. The lower detection limit of the method under the present configuration was 5 nmol L^{-1}. Vertical CH_4 fluxes through the water column and the net methane production rate (NMPR) within the water column were derived from the estimation of turbulent diffusion of CH_4 across the concentration gradient according to the method established previously (Kankaala et al., 2006), also described in the Supplementary material.

As it will be shown in the results and discussion section, we observed in all lakes that the epilimnion and the hypolimnion were segregated by a layer of water column where dissolved CH_4 concentration was minimum. This layer, that acted as a buffer zone between hypo- and epilimnion, was called minimum methane zone (MMZ). From that observation, we characterized the CH_4 mass balance with four parameters. First, the total CH_4 oxidation in the hypolimnion was established by integration of the NMPR over the entire hypolimnion depth, expressed per unit of lake area, and identified as r_{AOM} hereafter. Second, the vertical CH_4 exchange rate between the epilimnion and the MMZ was established from the maximal flux determined at the interface between both layers and identified as r_{MMZ} hereafter. Third, CH_4 and CO_2 fluxes from the lakes to the atmosphere were determined using the static chamber method at the surface of the lakes in a recirculation mode coupled to the UGGA (Gerardo-Nieto et al., 2017). These fluxes were included into the CH_4 mass balance and identified as r_{ATM} hereafter. Fourth, a mass balance over the epilimnion showed that r_{MMZ} and r_{ATM}, both being CH_4 output, must be compensated by an equivalent input. This input was also considered in the CH_4 mass balance, as the sum of r_{MMZ} and r_{ATM}, and identified as r_{EPI} hereafter. Details of the methods used to determine fluxes, r_{AOM}, r_{MMZ}, r_{epi} and r_{ATM} are provided in the Supplementary material.

2.3. Sampling and physicochemical analysis

Water samples (one from the oxic epilimnion and one from the anoxic hypolimnion) were collected at replicate points A and B in all lakes with a water sampler (2.2 L Van Dorn Bottle). Water samples were collected in the same way from eight different depths at point D in L2 (1, 2, 4, 5, 6, 8, 9, 10 m-depth). Superficial sediments were sampled using a mud-sampler. Water and sediment samples were kept at 4 °C for no >24 h prior to further processing.

The stable isotopes of dissolved methane (δ^{13}C-CH_4 and δD-CH_4) and dissolved inorganic carbon (δ^{13}C-DIC), dissolved organic and inorganic carbon concentrations, optical properties of dissolved organic matter, suspended solids, trace elements, major anion and cation concentrations, were analyzed in the water samples. The corresponding material and methods are described in Supplementary material.

2.4. Prokaryotic community analysis

2.4.1. Sample preparation and DNA extraction

After prefiltration at 80 μm (nylon net filters, Merck Millipore, Cork Ireland), water samples from each site were filtered at 0.22 μm (nitrocellulose GSWP membrane filters, Merck Millipore, Cork, Ireland) until filter clogging, i.e. after 275 to 1480 mL of flow through, depending on lake and depth. The 0.22-μm filter was frozen at −20 °C until DNA extraction. DNA was extracted from the water filters and the sediment with the PowerWater and PowerSoil DNA isolation kits, respectively (MoBIO Laboratories, Inc., Carlsbad, CA, USA). The DNA extracts were stored at −20 °C.

2.4.2. Quantitative PCR

The abundances of bacterial 16S rRNA gene (total Bacteria), archaeal 16S rRNA gene (total Archaea), *pmoA* gene (encoding the beta subunit of particulate methane monooxygenase, phylogenetic marker for MOB) and *mcrA* gene (encoding the alpha subunit of methyl coenzyme M reductase, phylogenetic marker for methanogens and ANMEs) were estimated by quantitative PCR (qPCR). All measurements were performed in 20 μL duplicates with Takyon SYBR master mix (Eurogentec, Liège, Belgium) and 0.4 ng of template DNA, using a CFX96 thermocycler (Bio-Rad Laboratories, Hercules, CA, US). Primer sequences and concentrations, thermocycling conditions, and standard curve preparation are detailed in Supplementary Table S1.

2.4.3. 16S rRNA gene sequencing

The V4-V5 region of archaeal and bacterial 16S rRNA genes was amplified from the DNA extracts using 515F and 928R primers (GTGYCAGCMGCCGCGGTA and CCCCGYCAATTCMTTTRAGT) (Wang and Qian, 2009) and MTP Taq DNA polymerase (Sigma-Aldrich, Lyon, France). The thermocycling procedure was the following: 2 min denaturation at 94 °C, 30 cycles of 60 s at 94 °C for denaturation, 40 s at 65 °C for annealing and 30 s at 72 °C for elongation, followed by 10 min at 72 °C for final elongation. PCR products were sequenced using Illumina Miseq paired-end sequencing (2 × 250-bp). The nucleotide sequences have been deposited to the European Nucleotide Archive under BioProject code PRJEB36731, using the nomenclature detailed in Supplementary Table S2.

2.4.4. Bioinformatics and statistical analyses

After demultiplexing, the reads were merged using Flash (Magoc and Salzberg, 2011), with a minimum overlap between the forward and reverse sequences of 10 base pairs and maximum mismatch of 10% in the overlapping region (Lluch et al., 2015). The sequence dataset was then processed using the FROGS pipeline (Escudie et al., 2017). Briefly, sequences were denoised and Operational Taxonomic Units (OTUs) were identified using Swarm (Mahé et al., 2014). Chimera sequences were then removed using vsearch. OTUs that were below 0.005% of the total abundance across the sample set were removed, as previously recommended (Bokulich et al., 2013). A taxonomic affiliation was assigned to each OTU using Blast (Altschul et al., 1990) against SILVA 132 (Pintail 80) rRNA database (Quast et al., 2013).

The OTU sequences of methanogenic Archaea and MOB were extracted. For methanogens, OTUs belonging to the following lineages were considered: Methanomicrobia, Methanococci, Methanobacteria, Methanopyri and Verstraetearchaeia classes, and Methanomassiliicoccales and Methanofastidiosales orders. For aerobic MOB, OTUs belonging to the following lineages were considered: *Methylococcaceae*, *Methylomonadaceae*, *Methylothermaceae* and *Methylacidiphilaceae* families, *Methylobacterium*, *Methylocapsa*, *Methylocella*, *Methylocystis*, *Methyloferula*, *Methylosinus* and *Methylovirgula* genera.

Two phylogenetic trees were constructed, one for aerobic MOB (including 15 MOB OTUs from this study), and one for methanogens/ANME (including 14 OTUs from this study). In these phylogenetic trees we included 45 and 43 reference sequences from the SILVA 132 database (Quast et al., 2013), representative of methanogens/ANME and MOB lineages, respectively. In addition, we included the two best environmental matches to our OTUs in BLAST. The selected OTUs and the reference sequences were aligned using SeaView 4 (Gouy et al.,

2010) and maximum-likelihood phylogenetic trees were reconstructed using PhyML version 3 (Guindon and Gascuel, 2003).

All statistical analyses were conducted in R 3.4.3, using the vegan (Oksanen et al., 2013) and Phyloseq (McMurdie and Holmes, 2013) packages. The OTU abundance matrix was normalized by rarefying to the lowest number of reads per sample (9105). Alpha diversity was assessed through the calculation of observed richness and Simpson index. The depth effect on alpha diversity indexes was evaluated by ANOVA (*aov* function). The distribution of OTUs across lakes and depths was then analyzed by Principal Component Analysis (PCA), using the *rda* function. The clustering significance according to relative water depth was tested by non-parametric permutational multivariate analysis of variance (PERMANOVA) using Bray Curtis distance matrix with the *adonis* function. The first 50 OTUs with the highest variance were identified by using the score/species biplot representation. The significant correlation of selected OTUs with the ordination scores was tested by the *envfit* function. The most discriminant OTUs explaining the sample distribution in the PCA ordination (i.e. with p-value < 0.012) were selected and represented on the biplot. The table of environmental variables (Supplementary Table S3) was normalized (centered and scaled) in order to test for correlations with community ordination. Collinearity between environmental variables was tested by computing the pairwise Spearman correlation matrix. No significant correlation was found ($|r| > 0.9$, p-value < 0.05). The linear correlation between the PCA ordination of the microbial communities and the 25 independent environmental parameters was investigated using the *envfit* function. Fitted environmental vectors were represented on the PCA by arrows pointing to the direction of the increasing gradient. The arrows length is proportional to the correlation coefficient between the variable and the ordination. The significance of each correlation was assessed by permutation tests and only the 11 variables with p-value < 0.05 were displayed. The OTUs that were differentially distributed between AOM, MMZ and oxic layer were statistically identified by *DESeq2* (with p-value threshold fixed at 0.001), run on un-normalized sequence counts after removing rare OTUs (abundance sum on the 24 samples < 0.1%). The pairwise comparisons between AOM/MMZ, AOM/oxic layer and MMZ/oxic layer led to the identification of 33, 63 and 38 OTUs, respectively, yielding to 81 unique OTUs. The relative abundance (log-transformed) of these 81 differential OTUs was visualized on a heatmap (*heatmap.2* function). The 81 OTUs and the 24 samples were arranged by hierarchical clustering on the basis of their differential abundance patterns, using Bray-Curtis distance and complete method for dendrogram representation. In addition, the logarithmic fold change (log2FC) estimated for each OTU between two conditions was also represented on a heatmap. The taxonomy of the discriminant and differentially abundant OTUs was examined by Blast, and their correlation with the main MOB was assessed by Spearman correlation analysis.

3. Results and discussion

3.1. Evidence of CH_4 oxidation in anoxic water

The depth profiles of DO showed that the four lakes were oxygen-stratified at the time of sampling, with a clear oxycline and fully anoxic water underneath (Fig. 1). The oxycline was at 2.0, 2.5, 4.0 and 1.5 m depth in L1, L2, L3, and L4, respectively. The lakes were also thermally stratified, with temperatures ranging from 3.4 to 3.9 °C in the anoxic hypolimnion and from 15.6 to 18.3 °C in the oxic epilimnion (see Supplementary Table S3). In the four lakes, the maximal dissolved CH_4 concentrations ranged between 1.11 mg L^{-1} (in L1) and 18.86 mg L^{-1} (in L3), just above the sediment and decreased to approximately 0.01 mg L^{-1} in the epilimnion (Fig. 1). The $\delta^{13}C$ signature of CH_4 ($\delta^{13}C\text{-}CH_4 = -79.2 \pm 5.4‰$) and apparent fractionation factor ($\alpha = 1.08 \pm 0.01$, Supplementary Table S3) revealed that CH_4 at the bottom of the four lakes originated mainly from hydrogenotrophic methanogenesis (Hornibrook et al., 2000; Whiticar and Faber, 1986). This was supported by the presence of methanogen communities in sediments and bottom water, which revealed that OTUs classified as acetoclastic methanogens (all in *Methanosaeta* genus in the present dataset) accounted for only 10 ± 8% of the methanogen communities in the sediment (Supplementary Fig. S1).

A general upward decrease of dissolved CH_4 concentration was observed in the hypolimnion of all lakes, with contrasted patterns between lakes, but all supporting evidences of AOM. First, a minimum methane zone (MMZ) was observed in all lakes; i.e., zone of the water column where dissolved CH_4 concentration was lower than in the epilimnion and the hypolimnion. The latter implies that a downward CH_4 flux at the bottom of the epilimnion and an upward CH_4 flux in the hypolimnion were observed, MMZ acting as a diffusional barrier, illustrated in Fig. 2. The existence of a diffusional barrier in stratified lakes has been previously suggested (DelSontro et al., 2018b; Peeters et al., 1996; Thalasso et al., 2020), segregating the CH_4 cycling in the oxic epilimnion from the hypolimnion dominantly anoxic. The segregation between the CH_4 cycling observed in the epilimnion and the hypolimnion was also evidenced by the stable isotopic signature, with significantly higher stable isotopic signature of CH_4 in the epilimnion ($\delta^{13}C\text{-}CH_4 = -47.8 \pm 7.3$, $p < 0.0001$, Kruskal-Wallis test) and lower fractionation factor ($\alpha = 1.04 \pm 0.01$, $p < 0.0001$) compared to the bottom of the lakes (Supplementary Table S3). These higher values of $\delta^{13}C\text{-}CH_4$ and lower α in the epilimnion might reflect a higher contribution of acetoclastic production of CH_4. Besides, the coupled increase of $\delta^{13}C\text{-}CH_4$ and $\delta^{2}H\text{-}CH_4$ (Supplementary Table S3) from the hypolimnion to the epilimnion also suggests a contribution of CH_4 oxidation to the epilimnion isotopic signature. The expected concentration profiles, assuming a simple diffusive flux from the bottom of the lakes to the MMZ, were clearly above the observed concentration profiles, in all lakes (Fig. 2A). Thus, a net CH_4 oxidation in the hypolimnion must be considered in order to explain the observed profiles. The existence of a diffusional barrier and AOM is particularly clear in L2, where CH_4 concentrations decreased to undetectable levels between 4 and 6.5 m depth, i.e. well below the oxycline (3 m). This interesting case of complete CH_4 mitigation in the anoxic layer is similar to that described in Lago di Cadagno (Milucka et al., 2015), Lake Zug (Oswald et al., 2016b), and Lake Lugano (Blees et al., 2014), all being large meromictic alpine lakes in Switzerland.

The analysis of CH_4 depth profile using a diffusion-reaction model (Kankaala et al., 2006) allowed to determine the NMPR, which once integrated over the entire hypolimnion and expressed per unit of lake area, gave an AOM rate ranging from 1.29 to 307 mg CH_4 m^{-2} h^{-1}, identified as r_{AOM} in Fig. 2 (see below). These AOM rates were higher in lakes showing higher maximum CH_4 concentrations (L3, L4). Interestingly, the rate of methane oxidation measured by van Grinsven et al. (2020) in laboratory incubations was also maximal in the anoxic water of lake Lacamas (27.6 mg m^{-3} h^{-1}) and falls into our range. The CH_4 oxidation observed in the hypolimnion raises the important question of the oxic or anoxic nature of the process, although several arguments support AOM. First, the hypolimnetic CH_4 oxidation was found well below the oxycline and the maximum CH_4 oxidation activity was always observed several meters below the oxycline (2.9 to 5.2 m below), except in L3, where the maximum CH_4 oxidation took place 0.5 m below the oxycline. Thus, where CH_4 oxidation was observed, the DO availability was, at the most, inferior to 10 μg L^{-1}; i.e., detection limit of the probe, and probably much lower. Second, assuming a DO transfer from the upper layer of the water column, the rates of CH_4 oxidation from 1.29 to 307 mg CH_4

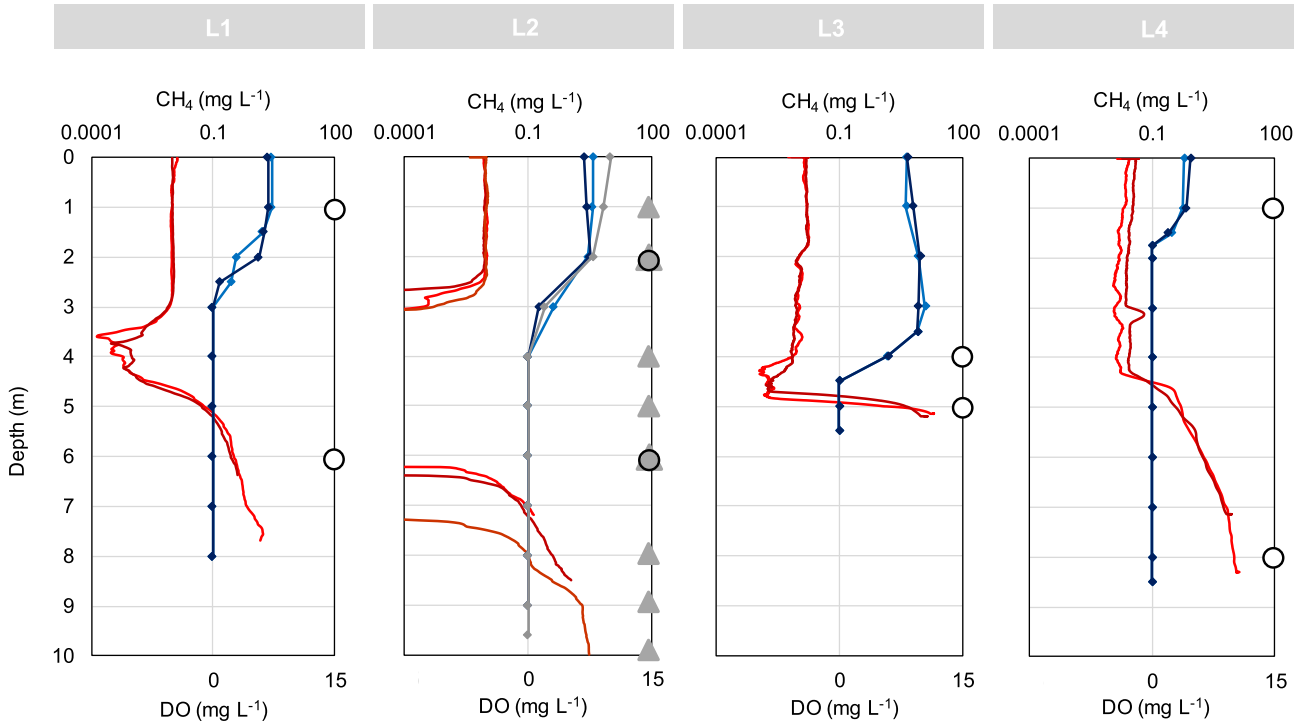

Fig. 1. Methane and oxygen profiles. Concentrations of dissolved CH_4 (red) and dissolved oxygen (DO, blue) along the water column of Siberian lakes L1 to L4. CH_4 profiles were obtained by independent measurements of field duplicates at some meters of distance (A, B) at the center of the lake, corresponding to the deepest zone of the lakes (light and dark red, respectively). In lake L2, an additional profile D is presented in a secondary basin of the lake (orange). DO profiles were measured at points A and B in all lakes (light and dark blue, respectively) and at additional point D in L2 (grey). For microbial ecology, field duplicates (A, B) of water samples were collected in the four lakes, at two depths (oxic and anoxic water), as indicated by the circles. In L2, additional water samples were collected with higher resolution at eight depths along profile D, as indicated by grey triangles.

$m^{-2}\ h^{-1}$ would have required a downward DO flux to the hypolimnion from 5.2 to 1230 mg $O_2\ m^{-2}\ h^{-1}$, according to the stoichiometry of 2 mol of O_2 required to oxidize 1 mol of CH_4. According to a maximum hypolimnetic diffusivity of $2.82 \times 10^{-3}\ m^2\ h^{-1}$ (Xing and Heinz, 1994), the DO concentration gradient along the water column, required to sustain aerobic methanotrophy, would have been from 2 to 430 mg L^{-1} per meter of water column depth, which is incompatible with the DO concentration inferior to 10 μg L^{-1} detected over the entire hypolimnion. Third, regarding the hypothesis of locally produced DO, the average rate of CH_4 oxidation expressed per unit of hypolimnion volume ranged 0.74–-1059 mg $m^{-3}\ h^{-1}$ and thus, would have required a DO local production from 2.9 to 4239 mg $m^{-3}\ h^{-1}$, which is from the higher range to several magnitude order above primary production reported for the epilimnion zones of 118 lakes (del Giorgio and Peters, 1993), thus unlikely to occur well below the oxycline in the four Siberian lakes presented here. Thus, based on these arguments, the CH_4 oxidation observed in the hypolimnion was assumed to be anaerobic. The same diffusion-reaction model allowed for the determination of the downward CH_4 flux, from the bottom of the epilimnion to the MMZ, identified as r_{MMZ} in Fig. 2. This parameter ranged 0–0.05 mg $CH_4\ m^{-2}\ h^{-1}$, thus representing a negligible amount of CH_4, compared to the AOM rates. Fluxes to the atmosphere were also quantified and ranged 0.08–1.05 mg $CH_4\ m^{-2}\ h^{-1}$ (identified as r_{ATM} in Fig. 2). The segregation of the epi- and hypolimnetic CH_4, is a clear evidence that the CH_4 emitted to the atmosphere was either produced locally under oxic conditions in the epilimnion (Bogard et al., 2014; Donis et al., 2017; Grossart et al., 2011) or laterally transported from the surrounding terrestrial ecosystem (DelSontro et al., 2018b). Altogether and assuming steady-state, the CH_4 lake budget indicates that AOM mitigated from 59.8 to 99.9% of the total CH_4 produced or imported in/to the lakes, while only the remaining fraction (0.1–40.2%) was emitted to the atmosphere (Fig. 2). This suggests that AOM is indeed a major component of the CH_4 cycle.

3.2. Depth-stratification of total prokaryotic communities

An overview of the taxonomic composition of all samples is displayed in Supplementary Fig. S1. A general description of the communities (prokaryotic abundance, number of sequences, percentage of Archaea, observed richness) is provided in Supplementary Table S2. There was a significant effect of relative sampling depth on alpha diversity, with higher observed richness and Simpson index in the anoxic hypolimnia ($p < 0.02$). The relationship between the microbial communities and the environmental variables were investigated by PCA ordination. The ordination accounted for 61.9% of total variance and showed that the communities from AOM hotspots shared high similarity among the four lakes. Microbial community structure was stratified along the depth of all four lakes (Fig. 3). With the exception of L3, total prokaryotic communities were significantly separated between oxic waters, MMZ and CH_4-rich anoxic waters where AOM occurred (PERMANOVA, $p < 0.002$). The separation of L3 communities may be due to notably distinct environmental parameters in this lake, such as higher pH, conductivity and DIC, as indicated by significant correlations found in the PCA analysis (Fig. 3A). Notably, L3 was the only CO_2-sink lake in this study (Supplementary Table S3), probably because of higher primary productivity. L3 communities were also characterized by higher fluorescence index (FI) and lower specific UV absorption (SUVA), indicative of higher primary productivity and relatively lower aromaticity of organic molecules.

A

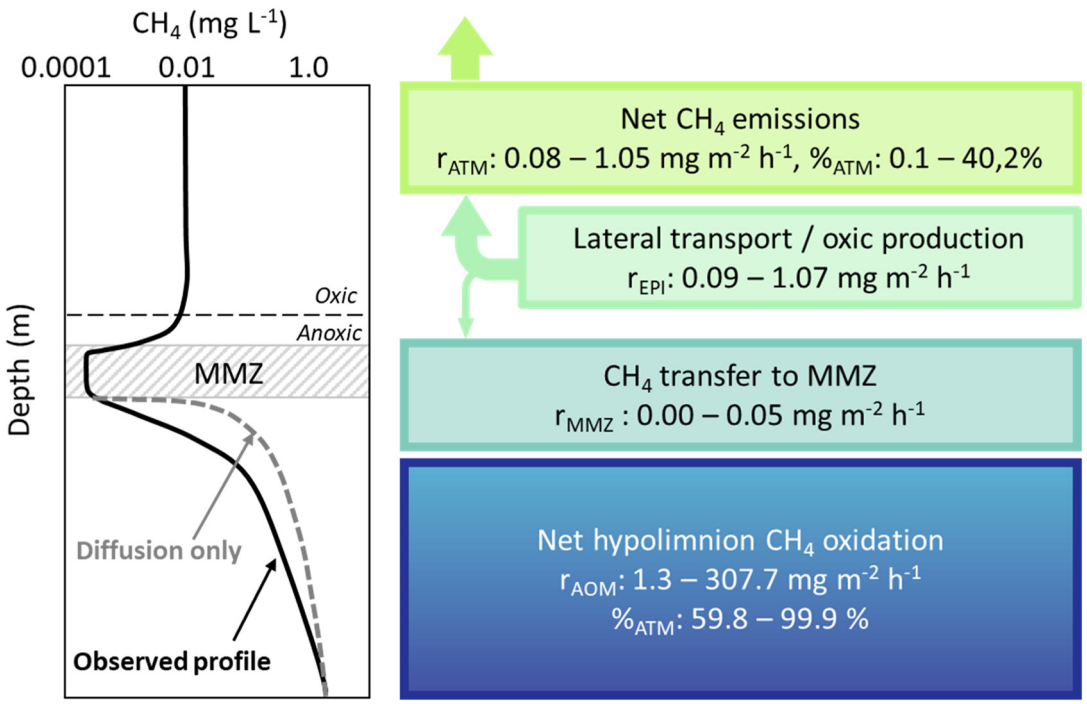

B

Lake	Max CH_4[1] (mg L^{-1})	AOM rate[2] (mg m^{-2} h^{-1})	Max AOM depth[3] (m)	Oxic layer depth[4] (m)	CH_4 emission[5] (mg m^{-2} h^{-1})	AOM contribution[6] (%)
1	0.38	8.8	6.9	3.0	1.05	89.3
2	0.05	1.3	7.7	4.0	0.87	59.8
3	7.94	307.7	5.0	4.5	0.67	99.8
4	9.43	114.4	7.2	1.8	0.08	99.9

Fig. 2. AOM contribution to the methane budget. (A) Conceptual sketch of the CH_4 concentration profiles observed in Siberian lakes, showing the diffusional barrier caused by minimum methane zone (MMZ, grey hatched area) and the deviation of the observed CH_4 profile from a simple linear diffusive gradient (please note the logarithmic scale). Boxes on the right indicate the magnitude of the biogeochemical processes involved. (B) Main parameters of the CH_4 biogeochemical cycle determined in four Siberian lakes. [1]Maximum dissolved CH_4 concentration. [2]Mean anaerobic methane oxidation (AOM) rate observed over the hypolimnion (r_{AOM}). [3]Depth at which the maximum peak of AOM was observed. [4]Depth at which dissolved oxygen was no longer detected. [5]CH_4 flux to the atmosphere (r_{ATM}). [6]Fraction of anaerobically oxidized CH_4, expressed as percent of the total CH_4 produced or imported in/to the lakes. Methods for r_{ATM}, r_{EPI}, r_{MMZ} and r_{AOM} determination are detailed in Supplementary material.

The prokaryotic communities in oxic waters were significantly correlated with higher temperature and redox conditions ($p < 0.001$), and were characterized by higher abundance of photosynthetic *Cyanobacteria* (Fig. 3B; $p < 0.009$). The community structure in anoxic water correlated significantly with higher contents of dissolved CH_4, Fe and Mn (Fig. 3A; $p < 0.05$).

3.3. ANME and Methylomirabilales are not major CH_4-oxidizers

In the depth profile of point D in L2, qPCR assays revealed a maximum abundance of archaea at the bottom of the lake (9.6 m), with archaeal 16S rRNA gene copy number reaching 2.5 ± 0.1% of the total prokaryotic 16S rRNA gene copy number (Fig. 4A). The *mcrA* gene also reached its maximum abundance at 9.6 m, with the copy numbers representing 0.57 ± 0.13% of the total prokaryotic community. However, within the maximal CH_4-oxidation zone (i.e. between 9 and 6.5 m), the *mcrA* gene was at the detection limit (<0.04% of the community), suggesting that neither ANME nor methanogens (through trace methane oxidation, Timmers et al., 2017) were involved in AOM in this lake.

ANME form lineages within the Methanomicrobia class. The phylogenetic comparison of reference ANME sequences and Methanomicrobia OTUs from the 16S rRNA gene sequencing confirmed that none of the OTUs detected in lakes 1, 2, 3 and 4 was closely related to ANME (Supplementary Fig. S2). The bacterial order Methylomirabilales, which includes the anaerobic methane oxidizer *Candidatus* Methylomirabilis, was not identified in the 16S rRNA gene libraries from any of the four lakes.

The qPCR and 16S rRNA gene sequencing approaches are both based on amplification reactions. PCR biases should be examined to avoid misinterpretations. The primer set targeting the *mcrA* gene for qPCR (mlas and mcrA-rev) fails to target ANME-2d sequences, as shown in Supplementary Table S4 and as previously reported (Vaksmaa et al., 2017). Nonetheless, this primer set has 100% coverage for the *mcrA* genes of other ANME lineages. The universal primer set used for 16S rRNA gene sequencing (515F and 928R) covered >98.5% of anaerobic methane oxidizers lineages: ANME-1a/1b, ANME-2a/2b, ANME-2c, ANME-2d and Ca. *Methylomirabilis* (Supplementary Table S4). Although the primers coverage was not 100% and was estimated on a limited number of taxonomically-affiliated sequences available in the databases, these analyses suggest it is unlikely that our combination of qPCR and sequencing approaches would miss major anaerobic methane oxidizers in this study.

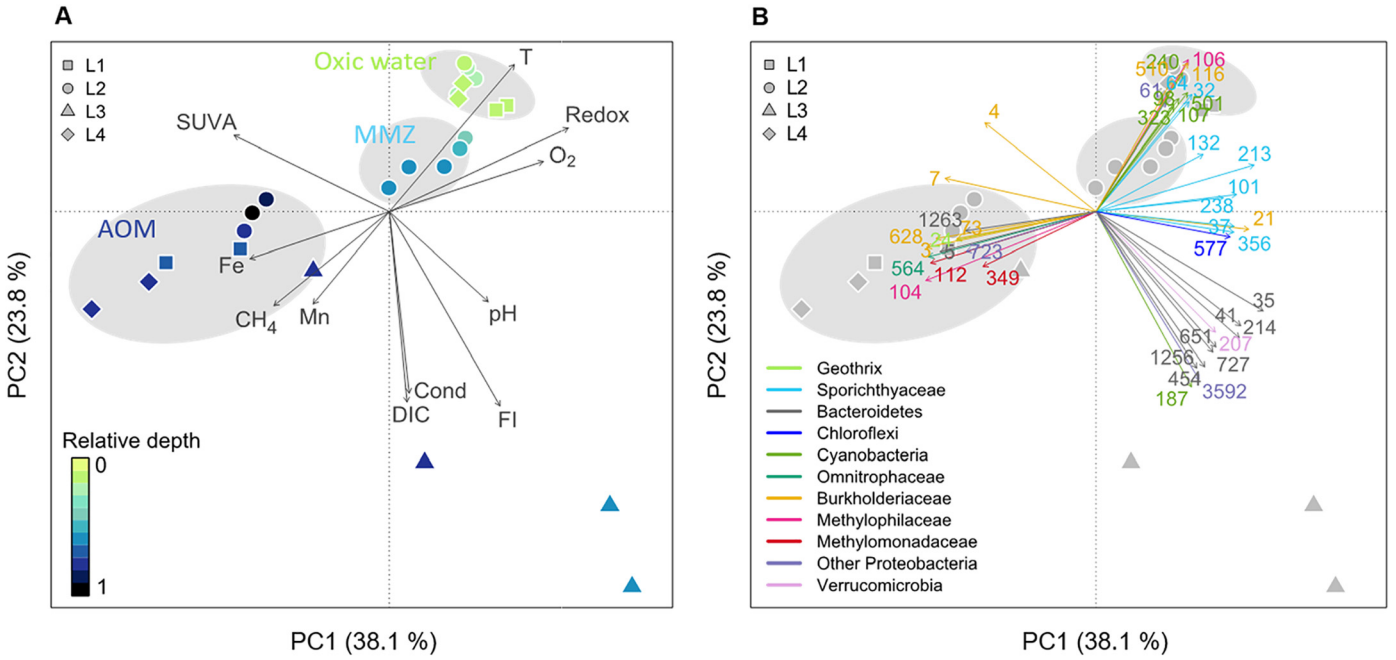

Fig. 3. Microbial community structure. (A) Principal Component Analysis (PCA) of the filtered and normalized OTU abundance table of microbial communities along the water column in the four Siberian lakes (L1 to L4, indicated by the symbol shape) at different relative sampling depths (as indicated by the color gradient). Ellipses represent significant depth-based clustering (p-value < 0.002 by non-parametric MANOVA), after excluding L3, showing community stratification between oxic water, MMZ (methane minimum zone) and AOM zone (anaerobic oxidation of methane). Significant correlations between ordination and environmental variables are represented (*envfit* function, p-value < 0.05) (SUVA: specific ultraviolet absorbance; Cond: conductivity; FI: fluorescence index; DIC: dissolved inorganic carbon; T: temperature). (B) Identification of the 42 most discriminant OTUs explaining the community distribution on the ordination (*envfit* function, p-value < 0.012) labeled with their OTU number. Arrow color represents the OTU taxonomic affiliation at the phylum, family or genus levels.

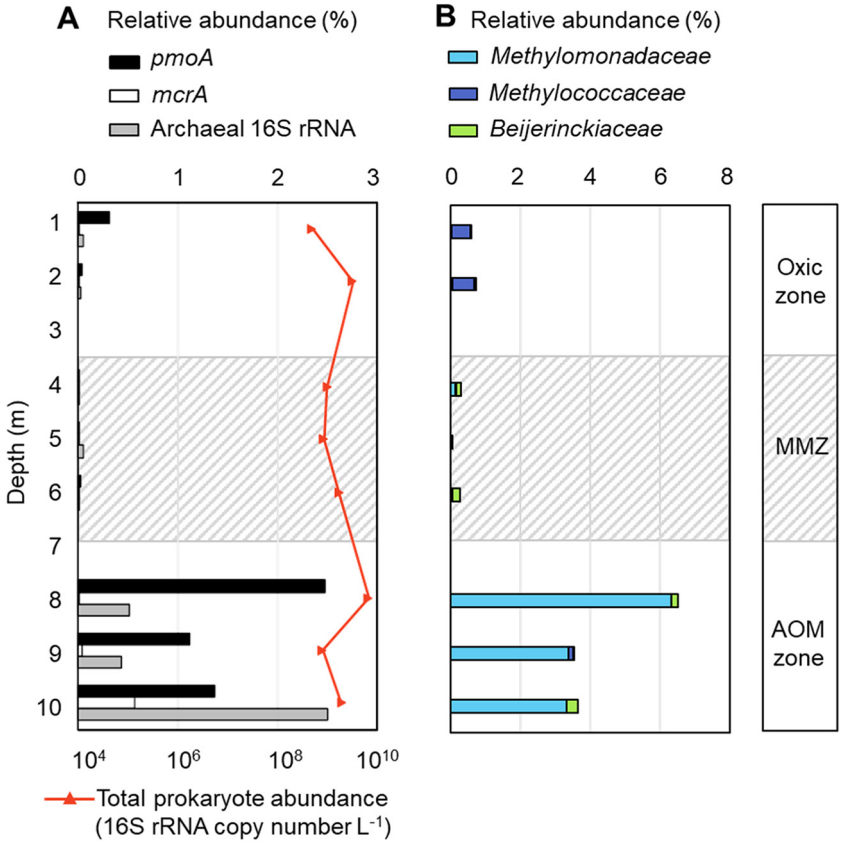

Fig. 4. | Methane oxidizing bacteria abundances. (A) Relative abundance of functional genes *pmoA*, *mcrA* and archaeal 16S rRNA gene, as determined by qPCR, along the water column of L2 lake, at point D (bar graph, see sampling point positions in Fig. 1). The absolute abundance of total prokaryotes (bacterial and archaeal 16S rRNA genes) per liter of filtered water is represented as a red line. (B) Relative abundance of three MOB families based on their taxonomic affiliation determined by 16S rRNA gene sequencing (MiSeq) along the water column of L2 lake, at point D. The separation of water layers according to their major CH4-cycling processes is represented on the right bar: oxic water, MMZ (minimum methane zone), AOM (anaerobic oxidation of methane).

Taken together, these results show that AOM in the anoxic waters of lakes L1, L2, L3 and L4 could not be attributed to ANMEs, methanogens, or members of Methylomirabilales.

3.4. Predominance of methane-oxidizing bacteria (MOB) in anoxic waters

MOB were more abundant in the AOM zones than in the oxic waters of all lakes (Table 1). Genes encoding the functional marker of MOB (*pmoA*) amounted to between 1.1 and 17.4% of the 16S rRNA gene counts in the AOM zones of all four lakes, which was 19 to 189 times higher than in the corresponding oxic waters (Table 1 and Fig. 4). In the 16S rRNA gene libraries, MOB OTUs represented from 3.6 to 21.8% of total prokaryotes in the AOM zone, which is 7 to 93 times higher than in the corresponding oxic waters of the four lakes (Table 1). Interestingly, in L2, the maximum MOB abundance (*pmoA*: 2.5% of total prokaryotes, and MOB OTUs: 6.5% of the community) was observed at 8 m depth, identified as the AOM hotspot (Fig. 2B).

The 16S rRNA gene sequencing revealed that MOB communities were not only stratified in terms of abundance but also in terms of composition (Fig. 4B). MOB OTUs in oxic water were dominated by a unique *Methylococcaceae* sequence (OTU_1717), affiliated to *Methyloparacoccus*, reaching 38–93% of the MOB in this layer. It is recognized that γ-MOB are often favored by low temperature (Sundh et al., 2005) and outcompete alphaproteobacterial MOB at low CH_4 and high DO (Amaral and Knowles, 1995; Chowdhury and Dick, 2013; Henckel et al., 2000), excluding MOB that oxidize atmospheric methane (Tveit et al., 2019).

In the MMZ of L2, the MOB community was small (< 0.3% of the total prokaryotes, Fig. 4). Alphaproteobacterial MOB from *Beijerinckaceae* dominated this small fraction (Fig. 4B) and all five *Beijerinckaceae* members (OTUs 4110, 6215, 6978, 7183 and 8644) were affiliated to *Methylobacterium*. Facultative methanotrophy capacity has been reported for *Methylobacterium organophilum* and *M. populi* (Patel et al., 1982; VanAken et al., 2004), but these observations were later contradicted (Semrau and Dispirito, 2011). Thus, although it is uncertain whether *Methylobacterium* spp. can oxidize CH_4, the observation of few obligate MOB in the MMZ was consistent with the undetectable levels of CH_4 in that water layer.

In the AOM zone of all lakes, where MOB were the most abundant, sequences affiliated to *Methylomonadaceae* (γ-proteobacteria) accounted for >91% of the MOB sequences. The prevalence of aerobic γ-MOB in sediments (He et al., 2012; Martinez-Cruz et al., 2017; Rissanen et al., 2017) or at the oxic/anoxic interface of the water column (Table 2) was reported previously. The ability of *Methylomonadaceae* to oxidize CH_4 in anoxic conditions was evidenced by incubation activity measurements coupled to DNA- or PLFA-stable isotope probing in sediment samples (Martinez-Cruz et al., 2017), or to fluorescence in situ hybridization and/or nanometer-scale secondary ion mass spectrometry in water (Oswald et al., 2015). However, in the water column, most studies reported maximal CH_4 oxidation activity (measured in incubations under in-situ O_2 concentration) at the oxycline or just above the oxycline (Table 2), concurring with maximal MOB abundance. Only two previous studies evidenced a maximum abundance of γ-MOB exclusively in anoxic water, together with maximal AOM activity

Table 1
Relative abundances of functional *pmoA* gene (quantified by qPCR) and methane oxidizing bacteria (MOB, based on their taxonomic affiliation determined by 16S rRNA gene sequencing), in the oxic water and at the AOM hotspot (anoxic water) of lakes L1, L2, L3, L4 (see sampling point positions in Fig. 1). The range obtained between replicate sampling points A and B is provided. In L2, the values refer to profile D which was sampled with higher resolution (depths 1 and 2 m in the oxic zone; depths 8, 9 and 10 m in the AOM zone).

		pmoA abundance (% of total prokaryotes)	MOB abundance (% of total reads)
L1	Oxic zone	0.09–0.42	0.41–0.45
	AOM zone	16.11–17.38	10.49–11.87
L2	Oxic zone	0.04–0.32	0.58–0.74
	AOM zone	1.12–2.47	3.56–6.51
L3	Oxic zone	0.08–0.09	0.11–0.12
	AOM zone	12.12–12.22	4.99–11.62
L4	Oxic zone	0.12–0.14	0.53–0.94
	AOM zone	2.33–2.53	20.36–21.76

(van Grinsven et al., 2020; Rissanen et al., 2018) (Table 2). Beyond these lines of evidence, the quantitative contribution of AOM to global lake CH_4 budget was rarely examined in combination with identification of microbial key players. AOM did not exceed one third of the CH_4 oxidation in the water column of the meromictic Lake Pavin, as estimated by reactive transport modelling of CH_4 (Lopes et al., 2011). To our knowledge, the significance of *Methylomonadaceae*-related AOM in CH_4 budget was not assessed, except in the present study (Table 2). Our results significantly contribute to the current knowledge by showing that the substantial and unprecedented anaerobic CH_4 mitigation in situ (AOM representing 60–100% of CH_4 budget) could be attributed to *Methylomonadaceae*.

3.5. Identification of Methylomonadaceae members as major methane oxidizers in anoxic waters

In order to address the ecology of *Methylomonadaceae* in these lake ecosystems we studied them at OTU level resolution. Ten OTUs were classified as belonging to *Mehylomonadaceae*, five of which were affiliated to the genus *Methylobacter* (OTUs 112, 601, 1638, 2841 and 20610), two to *Crenothrix* (OTUs 1925 and 2088) and three that were not assigned to a genus (OTUs 349, 351 and 3464; Fig. 5A). All ten were most similar to sequences retrieved from high-latitude or high-altitude ecosystems (Fig. 5B). The most abundant MOB OTUs in all lakes were OTUs 112 and 349 (Fig. 5C). Their maximum abundance was consistently found in the AOM hotspots. Furthermore, the changes

Table 2
Major outcomes from studies combining the assessment of anaerobic methane oxidation (AOM) activity and the identification of γ-MOB as major contributors in lake water. In bold: present study.

Lake	Method of AOM activity determination	Depth of maximal CH_4 oxidation activity[a]	Significance of AOM in CH_4 budget	Depth of maximal MOB abundance[b]	Predominant MOB in the water column at max. abundance depth	MOB identification and quantification methods	Reference
La Cruz	Incubations[c]	Oxycline/anoxic	–	Oxic	γ-MOB	CARD-FISH[d]	Oswald et al. (2016a)
Svetloe	Incubations[c]	Oxycline	–	Oxic	*Methylobacter*	16S rRNA gene sequencing	Kallistova et al. (2018)
Zug	Incubations[c]	Oxic	–	Oxic	γ-MOB	CARD-FISH[d]	Oswald et al. (2016b)[e]
	–	–	–	Oxycline	Methylococcales, mainly *Methylobacter*	16S rRNA and *pmoA* gene sequencing	Mayr et al. (2019)
di Cadagno	Incubations[c]	Oxic	–	Oxic	γ-MOB from *Methylomonadaceae*	CARD-FISH and *pmoA* sequencing	Milucka et al. (2015)
Pavin	Reactive transport modelling	Oxic/oxycline	26–33%	Oxic/Oxycline	*Methylobacter*	16S rRNA gene and transcript sequencing	Biderre-Petit et al. (2011); Lopes et al. (2011)
Rotsee	Incubations[c]	Oxycline	–	Oxycline/anoxic	γ-MOB	CARD-FISH[d]	Oswald et al. (2015)
	–	–	–	Oxycline/anoxic	Methylococcales, mainly *Crenothrix*	16S rRNA and *pmoA* gene sequencing	Mayr et al. (2019)
Brownie, Canyon	CH_4 stable carbon isotopy $\delta^{13}C_{CH4}$	Oxycline	–	Oxycline/anoxic	γ-MOB	16S rRNA gene sequencing	Lambrecht et al. (2019)[f]
Lacamas	Incubations[c]	Anoxic	–	Anoxic	*Methylobacter*	16S rRNA and *pmoA* gene sequencing, Metagenomics	van Grinsven et al. (2020)
Alinen-Mustajärvi	Incubations[c]	–	–	Anoxic	Ca. *Methyloumidiphilus alinensis*	16S rRNA gene sequencing	Rissanen et al. (2018)
Mekkojärvi	Incubations[c]	Anoxic	–	Anoxic	*Methylobacter*	16S rRNA gene and transcript sequencing	
L1 to L4	**Diffusion-reaction modelling**	**Anoxic**	**60–100%**	**Anoxic**	***Methylobacter* and other *Methylomonadaceae***	**16S rRNA gene sequencing, *pmoA* qPCR**	**This study**

[a] Only when a comparison is possible between oxic/anoxic depths, i.e. when methane oxidation was assessed at O_2 concentrations that are representative of in situ conditions for each depth. The slash (/) indicates that equivalent activities were found at different depths.
[b] The slash (/) indicates that equivalent abundances were found at different depths.
[c] Potential AOM measured using ^{13}C-CH_4 incubations under in-situ conditions (or ^{14}C-CH_4 incubations in the case of Kallistova et al., 2018), or without spiked substrate in the case of van Grinsven et al. (2020).
[d] CARD-FISH combined with nanoSIMS, targeting the following known CH_4-oxidizing groups: Gammaproteobacteria MOB (Mgamma84 and -705 probes), AOM-associated archaea (AAA, AAA-FW-641 and -834 probes), ANMEs (ANME-1-350, -2-538 probes).
[e] Similar in situ results were reported from three consecutive sampling years, however the complete profiles of MO activities and MOB abundances were only measured in 2013 samples: therefore, only the 2013 data are presented in the present Table.
[f] Only the complete campaigns (including both isotopy and microbial community analysis) are included in the present table.

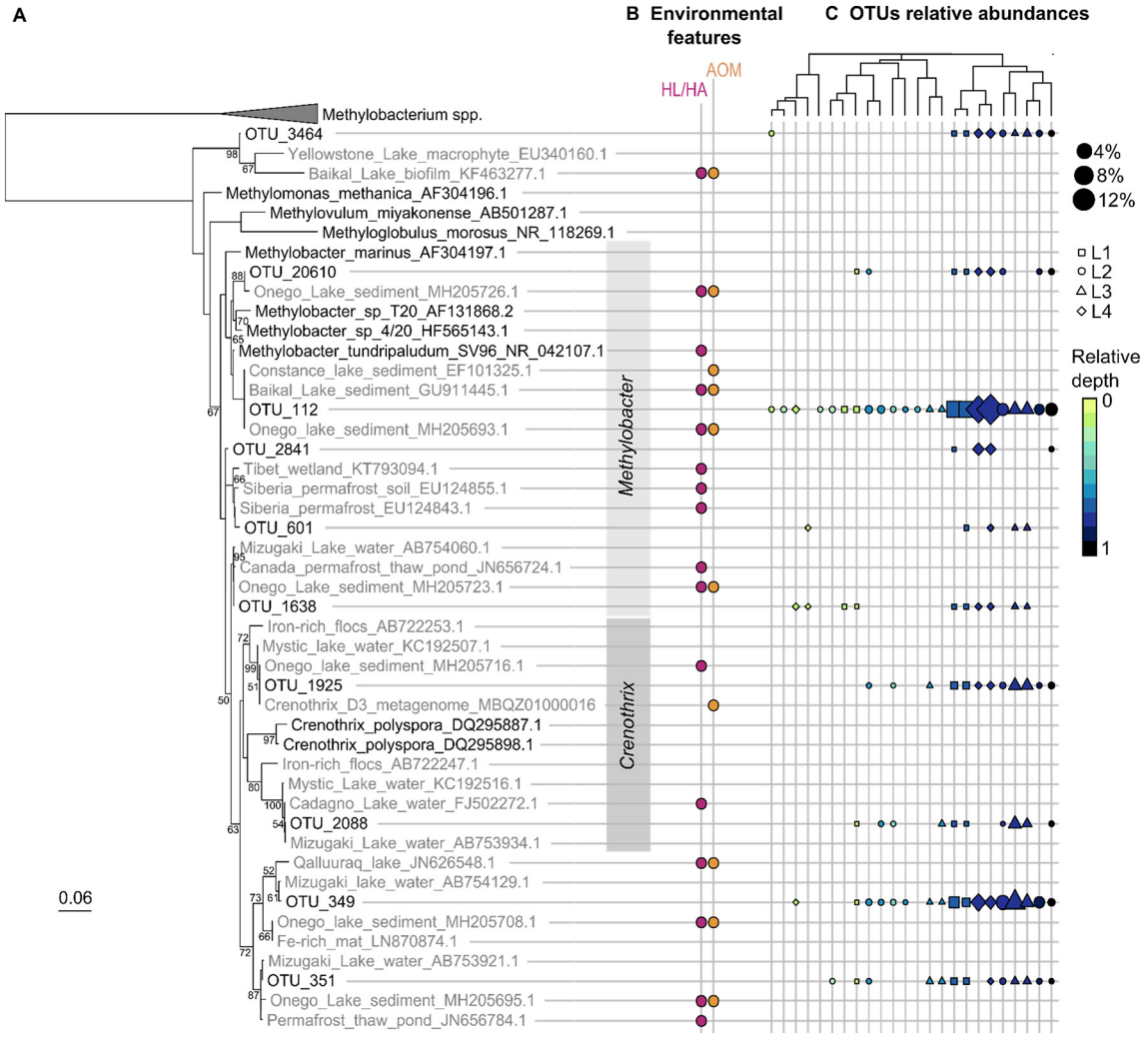

Fig. 5. *Methylomonadaceae* phylogenetic tree and abundances. (A) Phylogenetic tree of the ten partial 16S rRNA gene sequences retrieved from L1, L2, L3 and L4 affiliated to *Methylomonadaceae* family. OTUs affiliated to *Methylobacterium* genus (OTUs 4110, 6215, 6978, 7183, 8644) and 9 reference sequences from *Methylobacterium* spp. were used as outgroup. Bootstrap values > 50% are represented. The scale bar represents 6% sequence divergence. Bootstrap values were derived from 100 replicates. (B) Previous reports of environmental features are shown. "HL/HA" indicates that environmental samples or isolates originated from high-latitude (Arctic and Subarctic) or high-altitude (>1900 m) ecosystems. "AOM" indicates previous reports of anaerobic oxidation of methane in the same ecosystem and same environmental package (water/sediment) as the corresponding reference sequence. Note that this feature is not exhaustive: AOM might not have been reported in literature although effective. (C) Relative abundance of OTUs in water samples from the four lakes. Samples are ordered according to clustering based on Bray-Curtis distance using complete agglomeration method. Symbols are shaped according to the lake origin, and colored according to the relative sampling depth (0: water surface; 1: water/sediment interface). The symbol size is proportional to OTU relative abundance (percent of total prokaryotes).

in relative abundances of OTUs 112 and 349 contributed to the segregation of communities from AOM hotspots on the abundance pattern of differential OTUs (Fig. 6) and on the PCA ordination (p-value < 0.012; Fig. 3B), suggesting that CH_4 cycling shapes a large proportion of the microbial communities in these lakes.

OTU 112 was the overall most abundant MOB, representing 1.4 to 16.2% of the total number of sequences in the hypolimnia (Fig. 6). OTU 112 shared 99.5% sequence similarity with *Methylobacter tundripaludum* SV96 (NR_042107, closest cultured relative), which was isolated from Arctic wetland soil (Wartiainen et al., 2006) and identified as the most active MOB in anoxic arctic peat (Tveit et al., 2014). The OTU 112 sequence was identical (100% similarity) to sequences retrieved from sediments of large deep lakes: Lake Constance in Germany (EF101325), Lake Baikal in Siberia (GU911445) and Lake Onego in Russia (MH205693; Fig. 5B). AOM was observed in the sediments of these same lakes in other studies (Deutzmann et al., 2014; Pimenov et al., 2014; Thomas et al., 2018). Despite the different processes occurring in water and soil or sediment ecosystems, the main MOB OTUs found in the water column in this study have close relatives in wetland soil and sediment habitats. Furthermore, in the water column of several lakes, the genus *Methylobacter* was also the most abundant MOB at the oxic-anoxic transition (Table 2). Previously it was shown that phylotypes within *Methylobacter* can occupy different niches according to oxygen availability (Biderre-Petit et al., 2011).

While OTU 112 was most abundant, overall, OTU 349 outnumbered it in the anoxic water of L3 (up to 6.8% of the community). Interestingly, in lake L2, OTU 349 reached its maximum abundance at 8 m depth (3.7% of the community), just at the AOM hotspot (Figs. 2B, 6). OTU 349 had no close cultured relative. Its closest environmental sequence was derived from Lake Mizugaki water (AB754129, 99.7% similarity). OTU 349 shared 99.5% similarity with several environmental sequences from sediments of Lake Onego (MH205708), Fe-rich microbial mats (LN870874), ice covered Qalluuraq lake in Alaska (JN626674) and hypolimnion water from permafrost thaw pond in Canada (JN656780). Again, AOM activities were detected in most of these environments (He et al., 2012; Thomas et al., 2018).

OTU 1925, classified as *Crenothrix* sp., was present in the anoxic water of the four lakes, but at lower abundances than OTUs 112

Fig. 6. Left: Heatmap showing the relative abundance (log-transformed) of 81 OTUs identified by *DESeq2* as differentially abundant ($p < 0.001$) between the AOM, MMZ and oxic zones, in the four Siberian lakes (L1 to L4). Right: Heatmap showing the corresponding logarithmic fold change (log2FC) estimated for each OTU between two depth zones. Within each lake, the sampling point (field replicate) is indicated by the letter A, B or D, and the relative sampling depth (normalized by maximal depth) is indicated by the last numeric digits in the sample names. Samples and OTUs are arranged by hierarchical clustering on the basis of their differential abundance patterns, using Bray-Curtis distance. For each OTU, the taxonomic affiliation is provided at the genus level, or at the highest available level (f_: family; o_: order; c_: class; p_: phylum).

and 349 (<1.4% of the community). *Crenothrix* spp. are as-yet-uncultured multicellular and filamentous γ-MOB. Some *Crenothrix* were found to prefer oxygen-deficient niches (Mayr et al., 2019). Interestingly, Oswald et al. (2017, 2016b) demonstrated that γ-MOB in Lake Zug were active under oxic, sub-oxic and anoxic conditions. Despite their lower 16S rRNA gene abundance compared to other *Methylomonadaceae*, *Crenothrix* members were the major contributors to methane oxidation under oxygen-deficient conditions, as revealed by stable isotope labeling combined with nanoSIMS (Oswald et al., 2017).

Under hypoxia, AOM can be coupled to denitrification, within a single MOB organism, as experimentally confirmed in *Methylomonas denitrificans* (Kits et al., 2015b) and *Methylomicrobium album* strain BG8 (Kits et al., 2015a). Respiratory nitrate and nitrite reductases are encoded in over one third of Methylococcales genomes, including *Methylobacter* and *Crenothrix* species (Smith et al., 2018). Methane-dependent growth under nitrate-reducing conditions was experimentally demonstrated for *Crenothrix*, but evidence for in situ nitrate reduction is lacking (Oswald et al., 2017). In our study, it can be hypothesized that N-oxides could be used as electron acceptors by the three

predominant *Methylomonadaceae* MOB in the anoxic waters. Soluble nitrate concentration in the anoxic waters was below quantification limit (0.5 mg L^{-1} of $N\text{-}NO_3^-$) and nitrite concentration never exceeded 0.02 mg L^{-1} of $N\text{-}NO_2^-$ (Supplementary Table S3). Since N-oxides are extremely reactive intermediary species with high turnover (Zhu-barker et al., 2014), these low concentrations do not conclusively exclude nitrate or nitrite as electron acceptors.

3.6. Potential redox partnerships with Methylomonadaceae for performing AOM

The most significant discriminant OTUs (i.e. explaining community segregation along depth) were identified on the PCA (Fig. 3B) and the differentially abundant OTUs between AOM, MMZ and oxic zones were identified by DESeq2 (Fig. 6). Both approaches gave highly congruent results. Their taxonomy as well as their closest relatives are provided in Supplementary Table S5. Among these OTUs, the ones displaying significant correlation with the abundance of the main MOB OTUs (Spearman correlation coefficient > 0.75) were presented in Table 3. Such correlations give insights into co-occurrence and covariation of OTUS, but do not prove the existence of ecological interactions (Freilich et al., 2018; Peterson et al., 2020).

A high correlation was observed between the relative abundance of the main *Methylomonadaceae* and the discriminant *Methylophilaceae* OTU 104 (Table 3, Supplementary Table S5), with 100% identity to the facultative methylotroph *Methylotenera versatilis* (Kalyuzhnaya et al., 2012). The co-occurrence of γ-MOB and *Methylophilaceae* has been reported (He et al., 2015, 2012; Hernandez et al., 2015; Martinez-Cruz et al., 2017). OTU 104 could potentially serve as a partner for AOM by accepting electrons for N-oxides reduction, since the denitrification capacity of *Methylotenera* has been evidenced (Kalyuzhnaya et al., 2012; Oshkin et al., 2015).

In our ecosystems, several clues point at the coupling between CH_4- and Fe-cycles. In the AOM zone, the discriminant OTUs 3, 24 and 131 (Fig. 3, Supplementary Table S5, Table 3) co-occurring with the main *Methylomonadaceae*, were related to *Rhodoferax ferrireducens* (100% similarity), *Geothrix fermentans* (99.7%) and *Geobacter* sp. (99.2%), respectively, all recognized as Fe-reducers (Coates et al., 1999; Finneran et al., 2003; Holmes et al., 2007). The addition of Fe-oxides has been documented to effectively stimulate CH_4 oxidation by γ-MOB (Oswald et al., 2016b, 2016a), suggesting that Fe-reduction could shuttle the electrons produced by CH_4 oxidation. Total Fe concentrations were higher in the AOM zones (up to 3194 μg L^{-1}; Supplementary Table S3) and significantly correlated with the community structure ($p < 0.03$; Fig. 3A). The presumably important role of Fe in the anoxic water of the four lakes is supported by the significant correlation of the main *Methylomonadaceae* (OTUs 112 and 349) with OTUs 564 and 3251, identified as *Candidatus* Omnitrophus, which requires Fe for magnetosome biosynthesis (Kolinko et al., 2016). However, we acknowledge that measurements of Fe oxidation state would be needed to ascertain the availability of Fe-oxides.

Another possible way of coupling CH_4- and Fe-cycles relies on the regeneration of Fe-oxides that could serve subsequently as electron acceptors for AOM. OTUs 723, 313, 334 and 373 significantly co-occurred with the two main *Methylomonadaceae* (Table 3, Fig. 6). They were respectively related to *Gallionella capsiferriformans*, *Sediminibacterium*, *Sideroxydans lithotrophicus* and *Prolixibacteraceae*, recognized as Fe-oxidizing bacteria (Emerson, 2018; Fabisch et al., 2016, 2013; Iino et al., 2015; Li et al., 2015; Wang et al., 2012) (Supplementary Table S5). Oxidized compounds could also be regenerated through an interplay of biotic and abiotic cryptic reactions (Melton et al., 2014; Zhu-barker et al., 2014; Postma, 1985). Organic matter can also serve to fuel AOM, either directly as terminal electron acceptors, or indirectly to regenerate more common oxidants (Bai et al., 2019; Reed et al., 2017). Here, organic acids could be produced by fermentative bacteria such as OTUs 1220, 1263, 1387 (Supplementary Table S5, Table 3, Fig. 6).

Even if it is now recognized that *Methylomonadaceae* are not restricted to oxic environments, monooxygenases responsible for CH_4 oxidation catalysis do need oxygen. In the hypolimnion of the four lakes, oxygen might be present at concentrations below the detection limit (10 μg L^{-1}). On one hand, oxygen might be produced by oxygenic photosynthesis in apparently anoxic water. This hypothesis is supported by studies performed in the high-altitude meromictic Lago di Cadagno (Milucka et al., 2015) and in monomictic lake Rotsee (Oswald et al., 2015), which concluded that methane oxidation at similar depths (respectively 12 and 9 m) was light-dependent. In our study, sequences affiliated to oxygenic photosynthetic organisms accounted for 0.4 to 3.6% of the total sequences in hypolimnia samples, excluding L3 where they reached 26.9% (Fig. 6), distributed between *Cyanobiaceae* (19 to 86%) and chloroplastic sequences. None of these photosynthetic OTUs exhibited an abundance pattern positively correlated with the main MOB OTUs. Oxygenic photosynthesis might partially explain the observed methane oxidation in the four lakes, but we showed in paragraph 3.1 that photosynthetic activity would not be sufficient to aerobically oxidize the whole amount of CH_4. On the other hand, in the dark, biological intracellular dioxygen production has been documented through chlorite or nitric oxide dismutation (Ettwig et al., 2012) but, as previously mentioned, our dataset did not contain bacteria known to rely on nitric oxide dismutation for AOM, such as *Methylomirabilis*-like bacteria. Nevertheless, a wide phylogenetic diversity of NO dismutase (NOD) genes and homologues was recently found in various environments (Reimann et al., 2015; Zhu et al., 2017), suggesting that intracellular oxygen supplying is more widespread than previously thought.

4. Conclusion

In this study, the characterization of lake microbial communities in combination with high-resolution biogeochemical analyses were carried out to shed light on the water methane profiles observed in four Northern Siberian lakes. Three predominant γ-MOB, affiliated to *Methylobacter*, *Crenothrix* and unclassified *Methylomonadaceae*, were identified as potential key players in lake methane cycling, being highly abundant in the zones of maximum methane oxidation in the anoxic waters of the four lakes. The oxygen supply for fueling monooxygenase activity in *Methylomonadaceae* members residing in anoxic waters is still elusive, but hypolimnetic bacteria that co-occurred with the γ-MOB included putative Fe-oxidizing and Fe-reducing bacteria and denitrifying *Methylophilaceae*. This suggests that AOM could result from a tightly interacting microbiome, possibly through cryptic biogeochemical cycling involving aerobic MOB, denitrifiers and iron cycling microorganisms. More research is needed to ascertain that the microorganisms identified in this DNA-based study were really active in the four lakes and to unravel the metabolic interactions, e.g. through metatranscriptomics and/or stable isotope probing approaches. It was previously suggested that *Methylomonadaceae* might have a role in AOM in thermally stratified high-latitude or high-altitude lakes. Our study corroborates this idea and further indicates that *Methylomonadaceae*-driven AOM could be widespread among stratified lakes and has an important ecological function for the regulation of atmospheric GHG emissions.

Supplementary data to this article can be found online at https://doi.org/10.1016/j.scitotenv.2020.139588.

Data availability

The nucleotide sequences have been deposited to the European Nucleotide Archive under BioProject code PRJEB36731, using the nomenclature detailed in Supplementary Table S2. Access to the sequences and metadata is facilitated through the georeferenced mARS database (https://ipt.biodiversity.aq/resource?r=methanobase&v=1.4).

Table 3
Correlations between the relative abundance of the main MOB (OTUs 112 and 349) and the relative abundance of discriminant OTUs (identified on PCA and by differential analysis) in the AOM zone of the four Siberian lakes. The range of relative abundances in the four lakes and Spearman correlation coefficients are provided in the table. Only OTUs displaying correlation coefficient higher than 0.75 with at least one of the two MOBs were shown. All p-values were <0.002. The taxonomy of the discriminant OTUs was confirmed by Blast and their potential function inferred from literature (Supplementary Table S3).

Discriminant OTU number	Taxonomic identification	Putative function	Relative abundance (%)	Spearman correlation coefficient	
				OTU 112, *Methylobacter*	OTU 349, Unc. *Methylomonadaceae*
OTU 104[a]	*Methylotenera*	Methylotroph, denitrifier	0.0–12.3	0.85	0.87
OTU 24[a]	*Geothrix*	Fe-reducer	0.0–1.2	0.78	0.77
OTU 131[a]	*Geobacter*	Fe-reducer	0.0–2.4	0.74	0.85
OTU 313[a]	*Sediminibacterium*	Fe-oxidizer	0.0–1.3	0.75	0.81
OTU 334	*Sideroxydans*	Fe-oxidizer	0.0–1.0	0.75	0.87
OTU 373[a]	*Prolixibacteraceae*	Fe-oxidizer	0.0–1.0	0.73	0.78
OTU 723[a]	*Gallionella*	Fe-oxidizer	0.0–4.7	0.75	0.60
OTU 564[a]	Ca. *Omnitrophus*	Magnetotactic	0.0–1.7	0.76	0.80
OTU 3251	Ca. *Omnitrophus*	Magnetotactic	0.0–0.7	0.80	0.76
OTU 341	*Desulfatirhabdium*	Sulfate reducer	0.0–1.2	0.79	0.82
OTU 628[a]	*Bordetella*	Se-reducer, denitrifier	0.0–2.6	0.90	0.77
OTU 252	*Syntrophus*	Syntrophic VFA and aromatic compound oxidizer	0.0–1.3	0.73	0.77
OTU 1220	*Lentimicrobiaceae*	Fermentative	0.0–0.8	0.80	0.82
OTU 1263[a]	*Paludibacter*	Fermentative	0.0–1.5	0.82	0.73
OTU 1387	*Anaerovorax*	Fermentative	0.0–1.8	0.77	0.70
OTU 2469	*Alpinimonas*	Chemoorganotroph	0.0–1.1	0.82	0.73
OTU 3175	Ca. *Anammoximicrobium*	Anaerobic NH_4-oxidizer	0.0–0.9	0.86	0.80

[a] The OTUs marked by a star were identified by both correlation with PCA ordination (*envfit*) and differential abundance pattern (*DESeq2*); the others were only identified by differential abundance pattern (*DESeq2*), with the respective significance thresholds selected for each method.

CRediT authorship contribution statement

Léa Cabrol: Conceptualization, Investigation, Methodology, Supervision, Writing - original draft.**Frédéric Thalasso:**Conceptualization, Investigation, Formal analysis, Writing - review & editing.**Laure Gandois:**Methodology, Investigation, Writing - review & editing. **Armando Sepulveda-Jauregui:**Methodology, Investigation, Writing - review & editing.**Karla Martinez-Cruz:**Methodology, Investigation, Writing - review & editing.**Roman Teisserenc:**Resources.**Nikita Tananaev:**Resources.**Alexander Tveit:**Writing - review & editing. **Mette M. Svenning:**Writing - review & editing.**Maialen Barret:**Conceptualization, Investigation, Methodology, Supervision, Writing - original draft.

Declaration of competing interest

The authors declare that they have no known competing financial interests or personal relationships that could have appeared to influence the work reported in this paper.

Acknowledgement

We acknowledge MAEDI (Ministère des Affaires Etrangères et du Développement International) and MENESR (Ministère de l'Éducation nationale, de l'Enseignement supérieur et de la Recherche) French ministries and CONICYT (Comisión Nacional de Investigación Científica y Tecnológica) (Chile) for financial support through the ERANet-LAC joint program METHANOBASE (ELAC2014_DCC-0092). We are grateful to the University of Toulouse and Toulouse INP for supporting fieldwork costs through mobility programs. We also thank the Arctic Toulouse Initiative (Observatoire Midi-Pyrénées) for funding MiSeq sequencing. We are grateful to the Nutrition and Digestive Ecosystems team (INRA, Université de Toulouse, France) for library preparation prior to sequencing. We thank the GeT-PlaGe Genotoul platform for performing the MiSeq sequencing and for bioinformatics support. We thank the ECOS Sud-CONICYT Project "MATCH" C16B03 for mobility. We are grateful to Anatoli Pimov for field assistance. The authors thank F. Julien, V. Payre-Suc and D. Lambrigot for DOC and major elements analysis (PAPC platform, EcoLab laboratory), and I. Moussa and D. Dalger for $\delta^{13}C$-analysis of DIC (SHIVA platform). We are grateful to Dr. Daan Speth for providing reference *mcrA* sequences in each ANME lineage, derived from a phylogeny analysis.

References

Altschul, S., Gish, W., Miller, W., Myers, E., Lipman, D., 1990. Basic local alignment search tool. J. Mol. Biol. 403–410.
Amaral, J.A., Knowles, R., 1995. Growth of methanotrophs in methane and oxygen counter gradients. FEMS Microbiol. Lett. 126, 215–220.
Bai, Y.-N., Wang, X.-N., Wu, J., Lu, Y.-Z., Fu, L., Zhang, F., et al., 2019. Humic substances as electron acceptors for anaerobic oxidation of methane driven by ANME-2d. Water Res. 164, 114935. https://doi.org/10.1016/j.watres.2019.114935.
Barnes, R.O., Goldberg, E.D., 1976. Methane production and consumption in anoxic marine sediments. Geology 4, 297–300. https://doi.org/10.1130/0091-7613.
Bastviken, D., Cole, J.J., Pace, M.L., Van De Bogert, M.C., 2008. Fates of methane from different lake habitats: connecting whole-lake budgets and CH 4 emissions. J. Geophys. Res. 113, G02024. https://doi.org/10.1029/2007JG000608.
Biderre-Petit, C., Jézéquel, D., Dugat-Bony, E., Lopes, F., Kuever, J., Borrel, G., et al., 2011. Identification of microbial communities involved in the methane cycle of a freshwater meromictic lake: methane cycle in a stratified freshwater ecosystem. FEMS Microbiol. Ecol. 77, 533–545. https://doi.org/10.1111/j.1574-6941.2011.01134.x.
Blees, J., Niemann, H., Wenk, C.B., Zopfi, J., Schubert, C.J., Kirf, M.K., et al., 2014. Micro-aerobic bacterial methane oxidation in the chemocline and anoxic water column of deep south-Alpine Lake Lugano (Switzerland). 59, 311–324. https://doi.org/10.4319/lo.2014.59.2.0311.
Boetius, A., 2019. Global change microbiology — big questions about small life for our future. Nat. Rev. Microbiol. 17, 331–332. https://doi.org/10.1038/s41579-019-0197-2.
Bogard, M.J., P a, del Giorgio, Boutet, L., Chaves, M.C.G., Prairie, Y.T., Merante, A., et al., 2014. Oxic water column methanogenesis as a major component of aquatic CH4 fluxes. Nat. Commun. 5, 5350. https://doi.org/10.1038/ncomms6350.
Bokulich, N.A., Subramanian, S., Faith, J.J., Gevers, D., Gordon, I., Knight, R., et al., 2013. Quality-filtering vastly improves diversity estimates from Illumina amplicon sequencing. Nat. Methods 10, 57–59. https://doi.org/10.1038/nmeth.2276.Quality-filtering.
Chadburn, S.E., Burke, E.J., Cox, P.M., Friedlingstein, P., Hugelius, G., Westermann, S., 2017. An observation-based constraint on permafrost loss as a function of global warming. Nat. Clim. Chang. 7, 340–345. https://doi.org/10.1038/NCLIMATE3262.
Chistoserdova, L., Lidstrom, M.E., 2013. Aerobic methylotrophic prokaryotes. In: Rosenberg, E., DeLong, E.F., Lory, S., Stackebrandt, E., Thompson, F. (Eds.), The Prokaryotes: Prokaryotic Physiology and Biochemistry. Springer Berlin Heidelberg, Berlin, Heidelberg, pp. 267–285. https://doi.org/10.1007/978-3-642-30141-4_68.
Chowdhury, T.R., Dick, R.P., 2013. Ecology of aerobic methanotrophs in controlling methane fluxes from wetlands. Appl. Soil Ecol. 65, 8–22. https://doi.org/10.1016/j.apsoil.2012.12.014.
Coates, J.D., Ellis, D.J., Gaw, C.V., Lovley, D.R., 1999. Geothrix fermentans gen. nov., a novel Fe(III)-reducing bacterium from a hydrocarbon-contaminated aquifer. Int. J. Syst. Bacteriol. 49, 1615–1622.

Cohen, J., Screen, J.A., Furtado, J.C., Barlow, M., Whittleston, D., Coumou, D., et al., 2014. Recent Arctic amplification and extreme mid-latitude weather. Nat. Geosci. 7, 627–637. https://doi.org/10.1038/ngeo2234.

DelSontro, T., Beaulieu, J.J., Downing, J.A., 2018a. Greenhouse gas emissions from lakes and impoundments: upscaling in the face of global change. Limnol. Oceanogr. 3, 64–75. https://doi.org/10.1002/lol2.10073.

DelSontro, T., del Giorgio, P.A., Prairie, Y.T., 2018b. No longer a paradox: the interaction between physical transport and biological processes explains the spatial distribution of surface water methane within and across lakes. Ecosystems 21, 1073–1087. https://doi.org/10.1007/s10021-017-0205-1.

Deutzmann, J.S., Stief, P., Brandes, J., Schink, B., 2014. Anaerobic methane oxidation coupled to denitrification is the dominant methane sink in a deep lake. Proceedings of the National Academy of Sciences USA 111, 18273–18278. https://doi.org/10.1073/pnas.1411617111.

Donis, D., Flury, S., Stöckli, A., Spangenberg, J.E., Vachon, D., McGinnis, D., 2017. Full-scale evaluation of methane production under oxic conditions in a mesotrophic lake. Nat. Commun. 8, 1661–1671. https://doi.org/10.1038/s41467-017-01648-4.

Emerson, D., 2018. The role of iron-oxidizing bacteria in biocorrosion: a review. Biofouling 34, 989–1000. https://doi.org/10.1080/08927014.2018.1526281.

Escudie, F., Auer, L., Bernard, M., Mariadassou, M., Cauquil, L., Vidal, K., et al., 2017. Sequence analysis FROGS: Find, Rapidly, OTUs with Galaxy Solution. Bioinformatics, 1–8 https://doi.org/10.1093/bioinformatics/btx791.

Ettwig, K.F., Butler, M.K., Le Paslier, D., Pelletier, E., Mangenot, S., Kuypers, M.M.M., et al., 2010. Nitrite-driven anaerobic methane oxidation by oxygenic bacteria. Nature 464, 543–548. https://doi.org/10.1038/nature08883.

Ettwig, K.F., Speth, D.R., Reimann, J., Wu, M.L., Jetten, M.S.M., Keltjens, J.T., 2012. Bacterial oxygen production in the dark. Front. Microbiol. 3, 273. https://doi.org/10.3389/fmicb.2012.00273.

Fabisch, M., Beulig, F., Akob, D.M., Küsel, K., 2013. Surprising abundance of Gallionella-related iron oxidizers in creek sediments at pH 4.4 or at high heavy metal concentrations. Front. Microbiol. 4. https://doi.org/10.3389/fmicb.2013.00390.

Fabisch, M., Freyer, G., Johnson, C.A., Büchel, G., Akob, D.M., Neu, T.R., et al., 2016. Dominance of Gallionella capsiferriformans and heavy metal association with Gallionella-like stalks in metal-rich pH 6 mine water discharge. Geobiology 14, 68–90. https://doi.org/10.1111/gbi.12162.

Finneran, K.T., Johnsen, C.V., Lovley, D.R., 2003. Rhodoferax ferrireducens sp. nov., a psychrotolerant, facultatively anaerobic bacterium that oxidizes acetate with the reduction of Fe (III). Int. J. Syst. Evol. Microbiol. 53, 669–673. https://doi.org/10.1099/ijs.0.02298-0.

Freilich, M.A., Wieters, E., Broitman, B.R., Marquet, P.A., Navarrete, S.A., 2018. Species co-occurrence networks: can they reveal trophic and non-trophic interactions in ecological communities? Ecology 99, 690–699. https://doi.org/10.1002/ecy.2142.

Gerardo-Nieto, O., Astorga-España, M.S., Mansilla, A., Thalasso, F., 2017. Initial report on methane and carbon dioxide emission dynamics from sub-Antarctic freshwater ecosystems: a seasonal study of a lake and a reservoir. Sci. Total Environ. 593–594, 144–154. https://doi.org/10.1016/j.scitotenv.2017.02.144.

del Giorgio, P.A., Peters, R.H., 1993. Balance between phytoplankton production and plankton respiration in lakes. Can. J. Fish. Aquat. Sci. 50, 282–289. https://doi.org/10.1139/f93-032.

Gonzalez-Valencia, R., Magana-Rodriguez, F., Gerardo-Nieto, O., Sepulveda-Jauregui, A., Martinez-Cruz, K., Walter Anthony, K., et al., 2014. In situ measurement of dissolved methane and carbon dioxide in freshwater ecosystems by off-axis integrated cavity output spectroscopy. Environ Sci Technol 48, 11421–11428. https://doi.org/10.1021/es500987j.

Gouy, M., Guindon, S., Gascuel, O., 2010. SeaView version 4: a multiplatform graphical user interface for sequence alignment and phylogenetic tree building. Mol. Biol. Evol. 27, 221–224. https://doi.org/10.1093/molbev/msp259.

Graf, J.S., Mayr, M.J., Marchant, H.K., Tienken, D., Hach, P.F., Brand, A., et al., 2018. Bloom of a denitrifying methanotroph, '*Candidatus* Methylomirabilis limnetica', in a deep stratified lake. Environ. Microbiol. 20, 2598–2614. https://doi.org/10.1111/1462-2920.14285.

van Grinsven, S., Sinninghe Damsté, J.S., Abdala Asbun, A., Engelmann, J.C., Harrison, J., Villanueva, L., 2020. Methane oxidation in anoxic lake water stimulated by nitrate and sulfate addition. Environ. Microbiol. 22, 766–782. https://doi.org/10.1111/1462-2920.14886.

Grossart, H.-P., Frindte, K., Dziallas, C., Eckert, W., Tang, K.W., 2011. Microbial methane production in oxygenated water column of an oligotrophic lake. Proc. Natl. Acad. Sci. U. S. A. 108, 19657–19661. https://doi.org/10.1073/pnas.1110716108.

Guindon, S., Gascuel, O., 2003. A simple, fast, and accurate algorithm to estimate large phylogenies. Syst. Biol. 52, 696–704. https://doi.org/10.1080/10635150390235520.

He, R., Wooller, M.J., Pohlman, J.W., Quensen, J., Tiedje, J.M., Leigh, M.B., 2012. Diversity of active aerobic methanotrophs along depth profiles of arctic and subarctic lake water column and sediments. The ISME Journal 6, 1937–1948. https://doi.org/10.1038/ismej.2012.34.

He, R., Wooller, M.J., Pohlman, J.W., Tiedje, J.M., Leigh, M.B., 2015. Methane-derived carbon flow through microbial communities in arctic lake sediments. Environ. Microbiol. 17, 3233–3250. https://doi.org/10.1111/1462-2920.12773.

Henckel, T., Roslev, P., Conrad, R., Mikrobiologie, È., 2000. Effects of O2 and CH4 on presence and activity of the indigenous methanotrophic community in rice field soil. Environ. Microbiol. 2, 666–679.

Hernandez, M.E., Beck, D.A.C., Lidstrom, M.E., 2015. Oxygen availability is a major factor in determining the composition of microbial communities involved in methane oxidation. PeerJ 3, e801. https://doi.org/10.7717/peerj.801.

Holmes, D.E., O'Neil, R.A., Vrionis, H.A., N'Guessan, L.A., Ortiz-Bernad, I., Larrahondo, M.J., et al., 2007. Subsurface clade of Geobacteraceae that predominates in a diversity of Fe(III)-reducing subsurface environments. ISME J 1, 663–677. https://doi.org/10.1038/ismej.2007.85.

Hornibrook, E.R.C., Longstaffe, F.J., Fyfe, W.S., 2000. Evolution of stable carbon isotope compositions for methane and carbon dioxide in freshwater wetlands and other anaerobic environments. Geochim. Cosmochim. Acta 64, 1013–1027. https://doi.org/10.1016/S0016-7037(99)00321-X.

Hugelius, G., Strauss, J., Zubrzycki, S., Harden, J.W., Schuur, E.A.G., Ping, C.-L., et al., 2014. Estimated stocks of circumpolar permafrost carbon with quantified uncertainty ranges and identified data gaps. Biogeosciences 11, 6573–6593. https://doi.org/10.5194/bg-11-6573-2014.

Iino, T., Ohkuma, M., Sakamoto, M., 2015. Prolixibacter denitrificans sp. nov., an iron-corroding, facultatively aerobic, nitrate-reducing bacterium isolated from crude oil, and emended descriptions of the genus Prolixibacter and Prolixibacter bellariivorans. Int. J. Syst. Evol. Microbiol. 65, 2865–2869. https://doi.org/10.1099/ijs.0.000343.

IPCC, 2013. Summary for policymarkers. In: Stocker, T., Qin, D., Plattner, G., Tignor, M., Allen, S., Boschung, J., et al. (Eds.), Climate Change 2013: The Physical Science Basis. Contribution of Working Group I to the Fifth Assessment Report of the Intergovernmental Panel on Climate Change, Cambridge, UK and NY, USA. Cambridge University Press, Cambridge, UK and NY, USA, pp. 1–1585.

Joye, S.B., 2012. Microbiology: a piece of the methane puzzle. Nature 491, 538–539.

Kallistova, A., Kadnikov, V., Rusanov, I., Kokryatskaya, N., Beletsky, A., Mardanov, A., et al., 2018. Microbial communities involved in aerobic and anaerobic methane cycling in a meromictic ferruginous subarctic lake. Aquat. Microb. Ecol. 82, 1–18. https://doi.org/10.3354/ame01878.

Kalyuzhnaya, M.G., Beck, D.A.C., Vorobev, A., Smalley, N., Kunkel, D.D., Lidstrom, M.E., et al., 2012. Novel methylotrophic isolates from lake sediment, description of Methylotenera versatilis sp. nov. and emended description of the genus Methylotenera. Int. J. Syst. Evol. Microbiol. 62, 106–111. https://doi.org/10.1099/ijs.0.029165-0.

Kankaala, P., Huotari, J., Peltomaa, E., Saloranta, T., Ojala, A., 2006. Methanotrophic activity in relation to methane efflux and total heterotrophic bacterial production in a stratified, humic, boreal lake. Limnol. Oceanogr. 51, 1195–1204. https://doi.org/10.4319/lo.2006.51.2.1195.

Khmelenina, V.N., Murrell, J.C., Smith, T.J., Trotsenko, Y.A., 2018. Physiology and biochemistry of the aerobic methanotrophs. In: Rojo, F. (Ed.), Aerobic Utilization of Hydrocarbons, Oils and Lipids, Handbook of Hydrocarbon and Lipid Microbiology. Springer Berlin Heidelberg AG, part of Springer Nature, pp. 1–25. https://doi.org/10.1007/978-3-319-39782-5_4-1.

Kits, K.D., Campbell, D.J., Rosana, A.R., Stein, L.Y., 2015a. Diverse electron sources support denitrification under hypoxia in the obligate methanotroph Methylomicrobium album strain BG8. Front. Microbiol. 6, 1072. https://doi.org/10.3389/fmicb.2015.01072.

Kits, K.D., Klotz, M.G., Stein, L.Y., 2015b. Methane oxidation coupled to nitrate reduction under hypoxia by the Gammaproteobacterium Methylomonas denitrificans, sp. nov. type strain FJG1. Environ. Microbiol. 17, 3219–3232. https://doi.org/10.1111/1462-2920.12772.

Knief, C., 2015. Diversity and habitat preferences of cultivated and uncultivated aerobic methanotrophic bacteria evaluated based on pmoA as molecular marker. Front. Microbiol. 6. https://doi.org/10.3389/fmicb.2015.01346.

Knittel, K., Boetius, A., 2009. Anaerobic oxidation of methane: progress with an unknown process. Annu. Rev. Microbiol. 63, 311–334. https://doi.org/10.1146/annurev.micro.61.080706.093130.

Kolinko, S., Richter, M., Glöckner, F.-O., Brachmann, A., Schüler, D., 2016. Single-cell genomics of uncultivated deep-branching magnetotactic bacteria reveals a conserved set of magnetosome genes: genomic analysis of an uncultivated multicellular magnetotactic prokaryote. Environ. Microbiol. 18, 21–37. https://doi.org/10.1111/1462-2920.12907.

Lambrecht, N., Katsev, S., Wittkop, C., Hall, S.J., Sheik, C.S., Picard, A., et al., 2019. Biogeochemical and physical controls on methane fluxes from two ferruginous meromictic lakes. Geobiology, gbi.12365 https://doi.org/10.1111/gbi.12365.

Li, X., Wang, H., Hu, C., Yang, M., Hu, H., Niu, J., 2015. Characteristics of biofilms and iron corrosion scales with ground and surface waters in drinking water distribution systems. Corros. Sci. 90, 331–339. https://doi.org/10.1016/j.corsci.2014.10.028.

Lluch, J., Servant, F., Pa, S., Valle, C., Vali, S., Kuchly, C., et al., 2015. The characterization of novel tissue microbiota using an optimized 16S metagenomic sequencing pipeline. PLoS One 10, e0142334. https://doi.org/10.1371/journal.pone.0142334.

Lopes, F., Viollier, E., Thiam, A., Michard, G., Abril, G., Groleau, A., et al., 2011. Biogeochemical modelling of anaerobic vs. aerobic methane oxidation in a meromictic crater lake (Lake Pavin, France). Appl. Geochem. 26, 1919–1932. https://doi.org/10.1016/j.apgeochem.2011.06.021.

Magoc, T., Salzberg, S.L., 2011. FLASH : fast length adjustment of short reads to improve genome assemblies Tanja Mago c. Bioinformatics 27, 2957–2963. https://doi.org/10.1093/bioinformatics/btr507.

Mahé, F., Rognes, T., Quince, C., de Vargas, C., Dunthorn, M., 2014. Swarm: robust and fast clustering method for amplicon-based studies. PeerJ 2, e593. https://doi.org/10.7717/peerj.593.

Martinez-Cruz, K., Leewis, M., Charold, I., Sepulveda-jauregui, A., Walter, K., Thalasso, F., et al., 2017. Anaerobic oxidation of methane by aerobic methanotrophs in sub-Arctic lake sediments. Sci. Total Environ. 607–608, 23–31. https://doi.org/10.1016/j.scitotenv.2017.06.187.

Mayr, M.J., Zimmermann, M., Guggenheim, C., Brand, A., Bürgmann, H., 2019. Niche partitioning of methane-oxidizing bacteria along the oxygen–methane counter gradient of stratified lakes. ISME J https://doi.org/10.1038/s41396-019-0515-8.

McGuire, A.D., Anderson, L.G., Christensen, T.R., Dallimore, S., Guo, L., Hayes, D.J., et al., 2009. Sensitivity of the carbon cycle in the Arctic to climate change. Ecol. Monogr. 79, 523–555.

McMurdie, P.J., Holmes, S., 2013. phyloseq: an R package for reproducible interactive analysis and graphics of microbiome census data. PLoS One 8, e61217. https://doi.org/10.1371/journal.pone.0061217.

Melton, E.D., Swanner, E.D., Behrens, S., Schmidt, C., 2014. The interplay of microbially mediated and abiotic reactions in the biogeochemical Fe cycle. Nat. Rev. Microbiol. 12, 797–809. https://doi.org/10.1038/nrmicro3347.

Milucka, J., Kirf, M., Lu, L., Krupke, A., Lam, P., Littmann, S., et al., 2015. Methane oxidation coupled to oxygenic photosynthesis in anoxic waters. The ISME Journal 9, 1991–2002. https://doi.org/10.1038/ismej.2015.12.

Myhre, G., Shindell, D., Bréon, F., Collins, W., Fuglestvedt, J., Huang, J., et al., 2013. Anthropogenic and natural radiative forcing. In: Stocker, T.F., Qin, D., Plattner, G.-K., Tignor, M., Allen, S.K., Boschung, J., Nauels, A., Xia, Y., Bex, V., Midgley, P.M. (Eds.), Climate Change 2013: The Physical Science Basis, Vol. Contribution of Working Group I to the Fifth Assessment Report of the Intergovernmental Panel on Climate Change. Cambridge University Press, Cambridge, United Kingdom and New York, NY, USA.

Oksanen, J., Blanchet, G., Kindt, R., Simpson, G.L., Solymos, P., Stevens, M.H.H., et al., 2013. vegan: Community Ecology Package. R Package Version 2.0-6.

Oshkin, I.Y., Beck, D.A., Lamb, A.E., Tchesnokova, V., Benuska, G., McTaggart, T.L., et al., 2015. Methane-fed microbial microcosms show differential community dynamics and pinpoint taxa involved in communal response. ISME J 9, 1119–1129. https://doi.org/10.1038/ismej.2014.203.

Oshkin, I.Y., Miroshnikov, K.K., Danilova, O.V., Hakobyan, A., Liesack, W., Dedysh, S.N., 2019. Thriving in wetlands: ecophysiology of the spiral-shaped methanotroph Methylospira mobilis as revealed by the complete genome sequence. Microorganisms 7, 683. https://doi.org/10.3390/microorganisms7120683.

Oswald, K., Milucka, J., Brand, A., Littmann, S., Wehrli, B., Kuypers, M.M.M., et al., 2015. Light-dependent aerobic methane oxidation reduces methane emissions from seasonally stratified lakes. PLoS One, e0132574 https://doi.org/10.1371/journal.pone.0132574.

Oswald, K., Jegge, C., Tischer, J., Berg, J., Brand, A., Miracle, M.R., et al., 2016a. Methanotrophy under versatile conditions in the water column of the ferruginous meromictic Lake La Cruz (Spain). Front. Microbiol. 7. https://doi.org/10.3389/fmicb.2016.01762.

Oswald, K., Milucka, J., Brand, A., Hach, P., Littmann, S., Wehrli, B., et al., 2016b. Aerobic gammaproteobacterial methanotrophs mitigate methane emissions from oxic and anoxic lake waters: methane oxidation in Lake Zug. Limnol. Oceanogr. 61, S101–S118. https://doi.org/10.1002/lno.10312.

Oswald, K., Graf, J.S., Littmann, S., Tienken, D., Brand, A., Wehrli, B., et al., 2017. Crenothrix are major methane consumers in stratified lakes. The ISME Journal 11, 2124–2140. https://doi.org/10.1038/ismej.2017.77.

Panganiban, A.T., Patt, T.E., Hart, W., Hanson, R.S., 1979. Oxidation of methane in the absence of oxygen in lake water samples. Appl. Environ. Microbiol. 37, 303–309. https://doi.org/10.1128/AEM.37.2.303-309.1979.

Parks, D.H., Chuvochina, M., Waite, D.W., Rinke, C., Skarshewski, A., Chaumeil, P., et al., 2018. A standardized bacterial taxonomy based on genome phylogeny substantially revises the tree of life. Nat. Biotechnol. 36, 4229. https://doi.org/10.1038/nbt.4229.

Patel, R.N., Hou, C.T., Laskin, A.I., Felix, A., 1982. Microbial oxidation of hydrocarbons: properties of a soluble methane monooxygenase from a facultative methane- utilizing organism, Methylobacterium sp. strain CRL-26. Appl. Environ. Microbiol. 44, 1130–1137.

Peeters, F., Wüest, A., Piepke, G., Imboden, D.M., 1996. Horizontal mixing in lakes. Journal of Geophysical Research: Oceans 101, 18361–18375. https://doi.org/10.1029/96JC01145.

Peterson, A.T., Soberón, J., Ramsey, J., Osorio-Olvera, L., 2020. Co-occurrence networks do not support identification of biotic interactions. Biodiv Inf 15, 1–10. https://doi.org/10.17161/bi.v15i1.9798.

Pimenov, N.V., Kalmychkov, G.V., Veryasov, M.B., Sigalevich, P.A., Zemskaya, T.I., 2014. Microbial oxidation of methane in the sediments of central and southern Baikal. Microbiology 83, 773–781. https://doi.org/10.1134/S0026261714060149.

Postma, D., 1985. Concentration of Mn and separation from Fe in sediments-I. Kinetics and stoichiometry of the reaction between biiessite and dissolved Fe(II) at 10 °C. Geochim. Cosmochim. Acta 49, 1023–1033.

Quast, C., Pruesse, E., Yilmaz, P., Gerken, J., Schweer, T., Glo, F.O., et al., 2013. The SILVA ribosomal RNA gene database project: improved data processing and web-based tools. Nucleic Acids Res. 41, 590–596. https://doi.org/10.1093/nar/gks1219.

Reed, D.C., Deemer, B.R., van Grinsven, S., Harrison, J.A., 2017. Are elusive anaerobic pathways key methane sinks in eutrophic lakes and reservoirs? Biogeochemistry 134, 29–39. https://doi.org/10.1007/s10533-017-0356-3.

Reimann, J., Jetten, M.S.M., Keltjens, J.T., 2015. Metal enzymes in "impossible" microorganisms catalyzing the anaerobic oxidation of ammonium and methane. In: PMH, Kroneck, Sosa Torres, M.E. (Eds.), Sustaining Life on Planet Earth: Metalloenzymes Mastering Dioxygen and Other Chewy Gases. 15. Springer International Publishing, Cham, pp. 257–313. https://doi.org/10.1007/978-3-319-12415-5_7.

Rissanen, A.J., Karvinen, A., Nyk, H., Peura, S., Kankaala, P., Tiirola, M., et al., 2017. Effects of alternative electron acceptors on the activity and community structure of methane-producing and consuming microbes in the sediments of two shallow boreal lakes. FEMS Microbiol. Ecol. 93, fix078. https://doi.org/10.1093/femsec/fix078.

Rissanen, A., Saarenheimo, J., Tiirola, M., Peura, S., Aalto, S., Karvinen, A., et al., 2018. Gammaproteobacterial methanotrophs dominate methanotrophy in aerobic and anaerobic layers of boreal lake waters. Aquat. Microb. Ecol. 81, 257–276. https://doi.org/10.3354/ame01874.

Saunois, M., Stavert, A.R., Poulter, B., Bousquet, P., Canadell, J.G., Jackson, R.B., et al., 2019. The global methane budget 2000–2017. Earth System Science Data https://doi.org/10.5194/essd-2019-128.

Schulz, M., Faber, E., Hollerbach, A., Schröder, H.G., Güde, H., 2001. The methane cycle in the epilimnion of Lake Constance. Arch. Hydrobiol. 151, 157–176. https://doi.org/10.1127/archiv-hydrobiol/151/2001/157.

Semrau, J.D., Dispirito, A.A., 2011. Facultative methanotrophy: false leads, true results, and suggestions for future research. FEMS Microbiol. Lett. 323, 1–12. https://doi.org/10.1111/j.1574-6968.2011.02315.x.

Shen, L., Ouyang, L., Zhu, Y., Trimmer, M., 2019. Active pathways of anaerobic methane oxidation across contrasting riverbeds. The ISME Journal 13, 752–766. https://doi.org/10.1038/s41396-018-0302-y.

Singh, B.K., Bardgett, R.D., Smith, P., Reay, D.S., 2010. Microorganisms and climate change: terrestrial feedbacks and mitigation options. Nat. Rev. Microbiol. 8, 779–790. https://doi.org/10.1038/nrmicro2439.

Smith, L.C., Sheng, Y., MacDonald, G.M., 2007. A first pan-Arctic assessment of the influence of glaciation, permafrost, topography and peatlands on northern hemisphere lake distribution. Permafrost Periglac Process 18, 201–208. https://doi.org/10.1002/ppp.581.

Smith, G.J., Angle, J.C., Solden, L.M., Borton, M.A., Morin, T.H., Daly, R.A., 2018. Members of the genus Methylobacter are inferred to account for the majority of aerobic methane oxidation in oxic soils from a freshwater wetland. MBio 9, e00815–e00818.

Strauss, J., Schirrmeister, L., Grosse, G., Fortier, D., Hugelius, G., Knoblauch, C., et al., 2017. Deep Yedoma permafrost: a synthesis of depositional characteristics and carbon vulnerability. Earth Sci. Rev. 172, 75–86. https://doi.org/10.1016/j.earscirev.2017.07.007.

Streletsky, D.A., Tananaev, N., Opel, T., Shiklomanov, N.I., Nyland, K.E., Streletskaya, I.D., et al., 2015. Permafrost hydrology in changing climatic conditions: seasonal variability of stable isotope composition in rivers in discontinuous permafrost. Environ. Res. Lett. 10, 95003. https://doi.org/10.1088/1748-9326/10/9/095003.

Sundh, I., Bastviken, D., Tranvik, L.J., 2005. Abundance, activity, and community structure of pelagic methane-oxidizing bacteria in temperate lakes. Appl. Environ. Microbiol. 71, 6746–6752. https://doi.org/10.1128/AEM.71.11.6746-6752.2005.

Tamas, I., Smirnova, A.V., He, Z., Dunfield, P.F., 2014. The (d)evolution of methanotrophy in the Beijerinckiaceae — a comparative genomics analysis. The ISME Journal 8, 369–382. https://doi.org/10.1038/ismej.2013.145.

Thalasso, F., Sepulveda-Jauregui, A., Gandois, L., Martinez-Cruz, K., Gerardo-Nieto, O., Astorga-España, M.S., et al., 2020. Sub-oxycline methane oxidation can fully uptake CH4 produced in sediments: case study of a lake in Siberia. Sci. Rep. 10, 3423. https://doi.org/10.1038/s41598-020-60394-8.

Thauer, R.K., 2010. Functionalization of methane in anaerobic microorganisms. Angew. Chem. Int. Ed. 49, 6712–6713. https://doi.org/10.1002/anie.201002967.

Thomas, C., Frossard, V., Perga, M., Tofield-, N., Hofmann, H., Dubois, N., et al., 2018. Lateral variations and vertical structure of the microbial methane cycle in the sediment of Lake Onego (Russia). Inland Waters, 1–22 https://doi.org/10.1080/20442041.2018.1500227.

Timmers, P.H.A., Welte, C.U., Koehorst, J.J., Plugge, C.M., Jetten, M.S.M., Stams, A.J.M., 2017. Reverse methanogenesis and respiration in methanotrophic archaea. Archaea 1654237.

Tveit, A.T., Urich, T., Svenning, M.M., 2014. Metatranscriptomic analysis of Arctic peat soil microbiota. Appl. Environ. Microbiol. 80, 5761–5772. https://doi.org/10.1128/AEM.01030-14.

Tveit, A.T., Hestnes, A.G., Robinson, S.L., Schintlmeister, A., Dedysh, S.N., Jehmlich, N., et al., 2019. Widespread soil bacterium that oxidizes atmospheric methane. Proc. Natl. Acad. Sci. U. S. A. 116, 8515–8524. https://doi.org/10.1073/pnas.1817812116.

Vaksmaa, A., Jetten, M.S.M., Ettwig, K.F., Lüke, C., 2017. McrA primers for the detection and quantification of the anaerobic archaeal methanotroph 'Candidatus Methanoperedens nitroreducens'. Appl. Microbiol. Biotechnol. 101, 1631–1641. https://doi.org/10.1007/s00253-016-8065-8.

Valentine, D.L., Reeburgh, W.S., Hall, R., 2000. New perspectives on anaerobic methane oxidation. Environ. Microbiol. 2, 477–484.

Valenzuela, E.I., Avendaño, K.A., Balagurusamy, N., Arriaga, S., Nieto-Delgado, C., Thalasso, F., et al., 2019. Electron shuttling mediated by humic substances fuels anaerobic methane oxidation and carbon burial in wetland sediments. Sci. Total Environ. 650, 2674–2684. https://doi.org/10.1016/j.scitotenv.2018.09.388.

VanAken, B., Peres, C.M., Doty, S.L., Yoon, J.M., Schnoor, J.L., 2004. Methylobacterium populi sp. nov., a novel aerobic, pink-pigmented, facultatively methylotrophic, methane-utilizing bacterium isolated from poplar trees (Populus deltoides 6 nigra DN34). Int. J. Syst. Evol. Microbiol. 54, 1191–1196. https://doi.org/10.1099/ijs.0.02796-0.

Vonk, J.E., Tank, S.E., Bowden, W.B., Laurion, I., Vincent, W.F., Alekseychik, P., et al., 2015. Reviews and syntheses: effects of permafrost thaw on Arctic aquatic ecosystems. Biogeosciences 12, 7129–7167. https://doi.org/10.5194/bg-12-7129-2015.

Wang, Y., Qian, P.-Y., 2009. Conservative fragments in bacterial 16S rRNA genes and primer design for 16S ribosomal DNA amplicons in metagenomic studies. PLoS One 4, e7401. https://doi.org/10.1371/journal.pone.0007401.

Wang, J., Krause, S., Muyzer, G., Meima-Franke, M., Laanbroek, H.J., Bodelier, P.L.E., 2012. Spatial patterns of iron- and methane-oxidizing bacterial communities in an irregularly flooded, riparian wetland. Front Microbio 3. https://doi.org/10.3389/fmicb.2012.00064.

Wartiainen, I., Hestnes, A.G., Mcdonald, I.R., Svenning, M.M., 2006. Methylobacter tundripaludum sp. nov., a methane-oxidizing bacterium from Arctic wetland soil on the Svalbard islands, Norway (78° N). Int. J. Syst. Evol. Microbiol. 56, 109–113. https://doi.org/10.1099/ijs.0.63728-0.

Whiticar, M.J., Faber, E., 1986. Methane oxidation in sediment and water column environments—isotope evidence. Org. Geochem. 10, 759–768. https://doi.org/10.1016/S0146-6380(86)80013-4.

Wik, M., Varner, R.K., Anthony, K.W., MacIntyre, S., Bastviken, D., 2016. Climate-sensitive northern lakes and ponds are critical components of methane release. Nat. Geosci. 9, 99–105. https://doi.org/10.1038/ngeo2578.

Winkel, M., Sepulveda-Jauregui, A., Martinez-Cruz, K., Heslop, J.K., Rijkers, R., Horn, F., et al., 2019. First evidence for cold-adapted anaerobic oxidation of methane in deep sediments of thermokarst lakes. Environ Res Commun 1, 021002. https://doi.org/10.1088/2515-7620/ab1042.

Xing, F., Heinz, S., 1994. Temperature and Dissolved Oxygen Simulations for a Lake With Ice Cover. St. Anthony Falls Hydraulic Laboratory, Retrieved from the University of Minnesota Digital Conservancy, Minnesota.

Yu, Z., Pesesky, M., Zhang, L., Huang, J., Winkler, M., Chistoserdova, L., 2020. A complex interplay between nitric oxide, quorum sensing, and the unique secondary metabolite tundrenone constitutes the hypoxia response in *Methylobacter*. MSystems 5, e00770–19. https://doi.org/10.1128/mSystems.00770-19 (/msystems/5/1/msys.00770-19.atom).

Zehnder, A.J.B., Brock, T.D., 1980. Anaerobic methane oxidation: occurrence and ecology. Appl. Environ. Microbiol. 39, 11.

Zhu, B., Bradford, L., Huang, S., Szalay, A., Leix, C., Weissbach, M., et al., 2017. Unexpected diversity and high abundance of putative nitric oxide dismutase (Nod) genes in contaminated aquifers and wastewater treatment. Applied & Environmental Microbiology 83, e02750–16.

Zhu-barker, X., Cavazos, A.R., Ostrom, N., Horwath, W., Glass, J., 2014. The importance of abiotic reactions for nitrous oxide production. Biogeochemistry 126, 251–267. https://doi.org/10.1007/s10533-015-0166-4.